SUPPLEMENTARY FIGURE and FIGURE LEGENDS

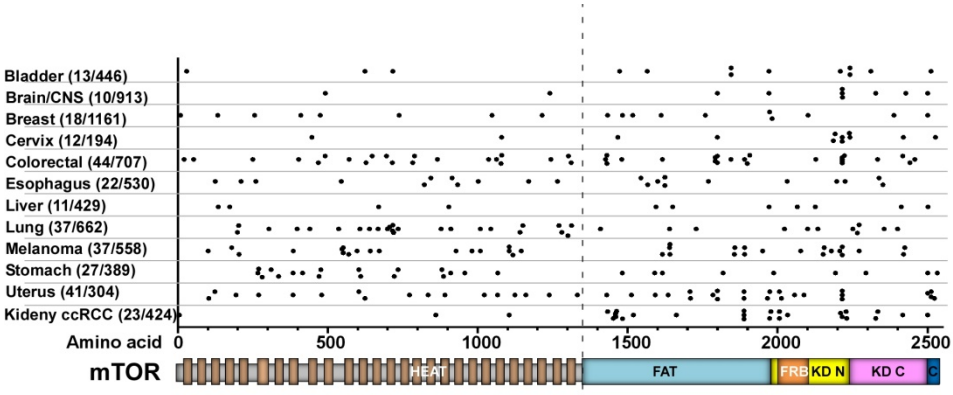

Supplementary Figure 1

Supplementary Figure 1 mTOR missense mutations reported in human cancer. Amino acid positions of mTOR missense mutations identified in different cancer types from TCGA studies were shown (adapted from cBioPortal). Numbers in the parenthesis indicate mTOR missense mutation versus total cases sequenced.

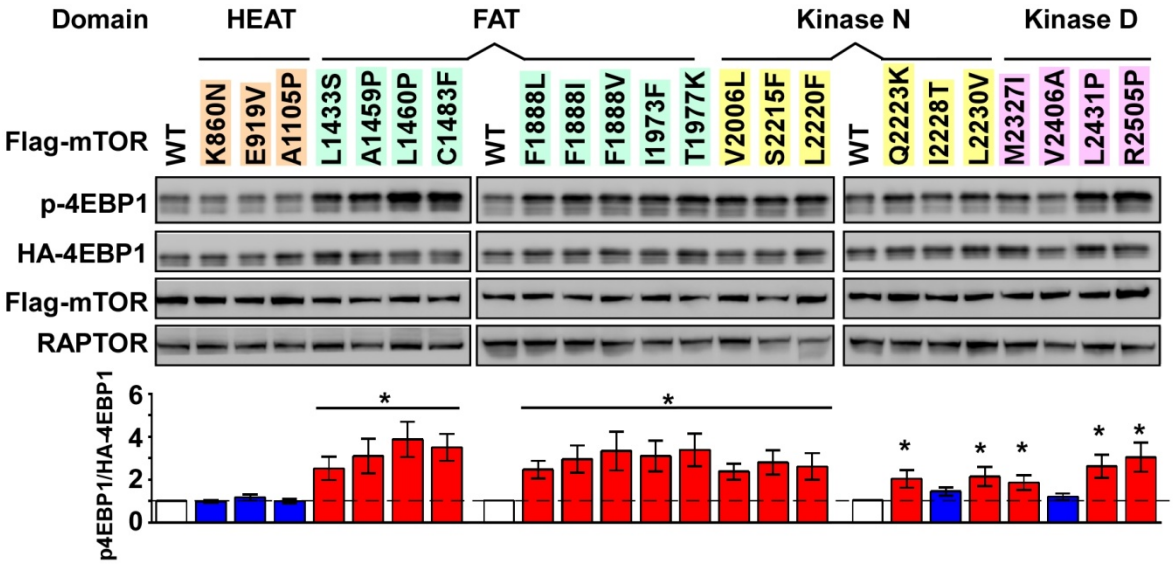

Supplementary Figure 2

Supplementary Figure 2 Most of the mTOR mutations in the FAT and kinase domains induce higher levels of 4EBP1 phosphorylation (S65) than WT mTOR. 293T cells were transfected with vectors expressing HA-tagged 4EBP1 and Flag-tagged WT or mutant mTOR. Whole cell lysates were subjected to immunoblot analysis using the indicated antibodies. Densitometry of phosphorylated 4EBP1 versus HA-4EBP1 from three independent experiments is shown (mean ± SEM, n=3 independent experiments). *, $P<0.05$ (*t*-test).

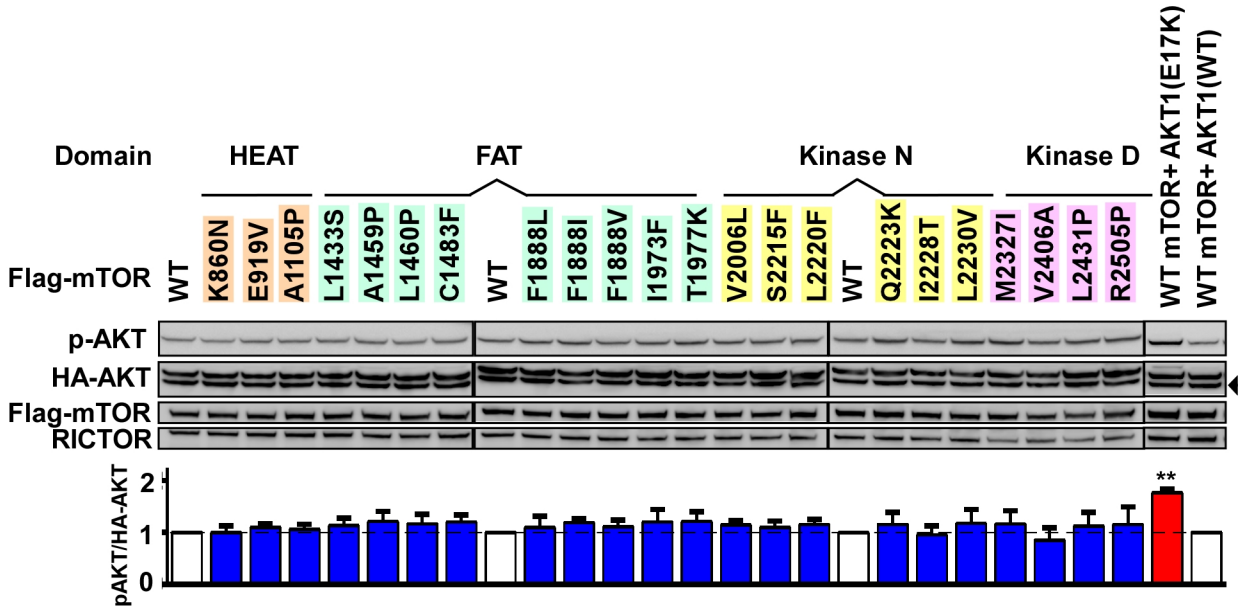

Supplementary Figure 3

Supplementary Figure 3 Most of the mTOR mutations in ccRCC do not induce higher levels of AKT phosphorylation (S473) than WT mTOR. 293T cells were transfected with vectors expressing HA-tagged AKT and Flag-tagged WT or mutant mTOR. For positive control, 293T cells were transfected with vectors expressing HA-tagged AKT1 or AKT1 activating mutation (E17K) and Flag-tagged WT. 36 hours later, cells were starved for serum overnight before harvest. Whole cell lysates were subjected to immunoblot analysis using the indicated antibodies. Densitometry of phosphorylated AKT (S473) versus HA-AKT from three independent experiments is shown (mean ± SEM, n=3 independent experiments). **,*P*<0.05 (*t*-test).

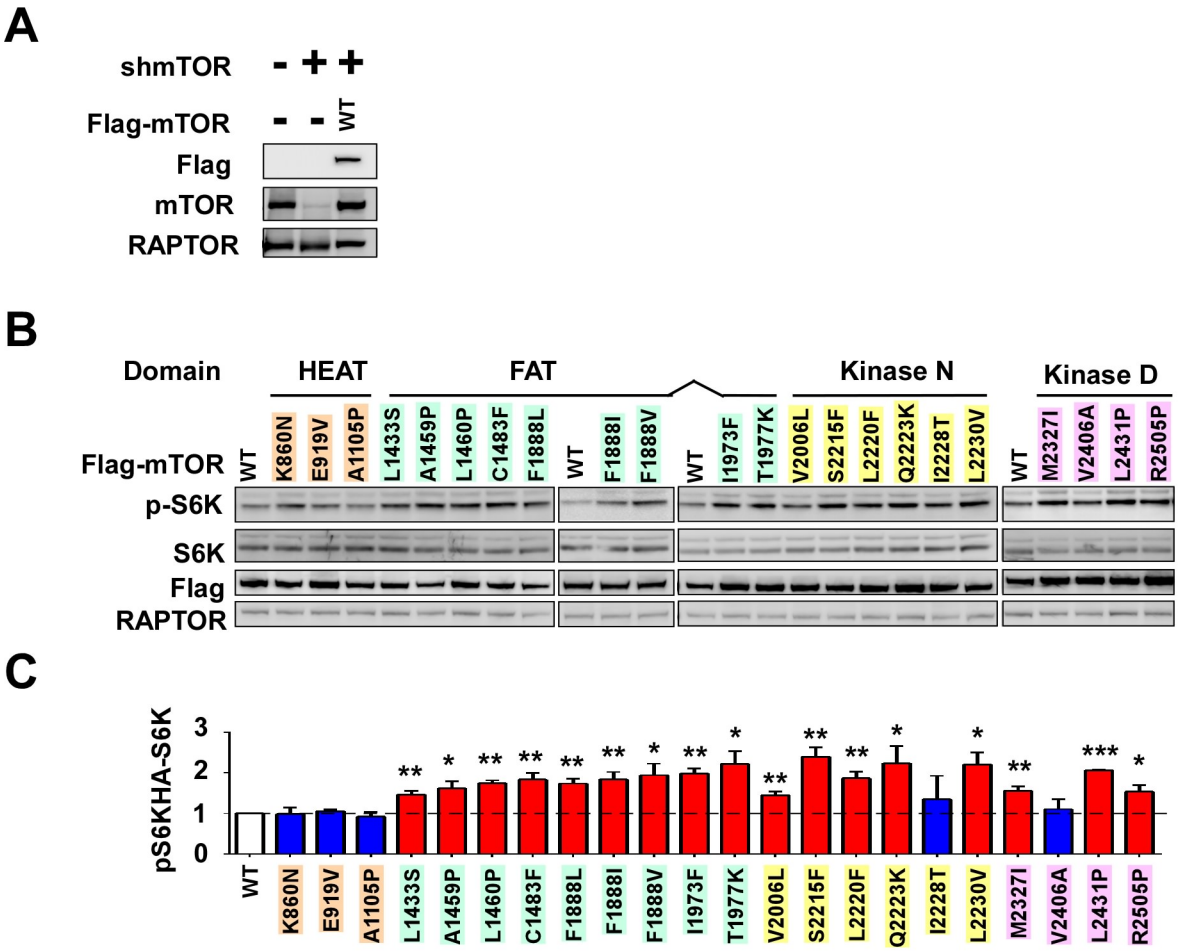

Supplementary Figure 4

Supplementary Figure 4 Most of the mTOR mutations in the FAT and kinase domains expressed at same level as endogenous protein induce higher levels of S6K phosphorylation (T389) than WT mTOR. (A) Expression of Flag-mTOR in mTOR-silenced 293T cells. 293T cells, mTOR-silenced (targeting 3'UTR region) 293T cells expressing Flag-mTOR were subjected to immunoblot analysis using the indicated antibodies. Of note, Flag-mTOR was expressed at a similar level as endogenous mTOR. **(B)** mTOR-silenced 293T cells were transfected with vectors expressing Flag-tagged WT or mutant mTOR. 48 hours post transfection, cells were lysed and whole cell lysates were subjected to immunoblot analysis using the indicated antibodies. **(C)** Densitometry of phosphorylated S6K (T389) versus S6K from three independent experiments is shown (mean ± SEM, n=3 independent experiments). * , P<0.1, ** , P<0.05, *** , P<0.01 (t-test).

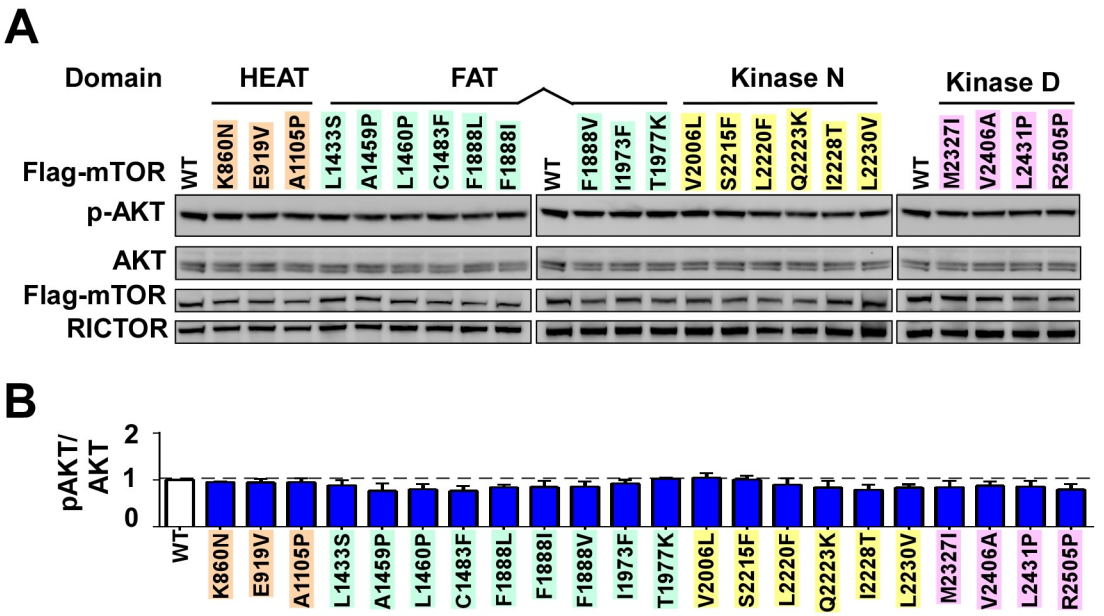

Supplementary Figure 5

Supplementary Figure 5 mTOR mutations expressed at comparable levels as endogenous protein do not induce higher levels of AKT phosphorylation (S473) than WT mTOR. (A) mTOR-silenced 293T cells were transfected with vectors expressing Flag-tagged WT or mutant mTOR. 48 hours post transfection, cells were lysed and whole cell lysates were subjected to immunoblot analysis using the indicated antibodies. **(B)** Densitometry of phosphorylated AKT (S473) versus AKT from three independent experiments is shown (mean ± SEM, n=3 independent experiments).

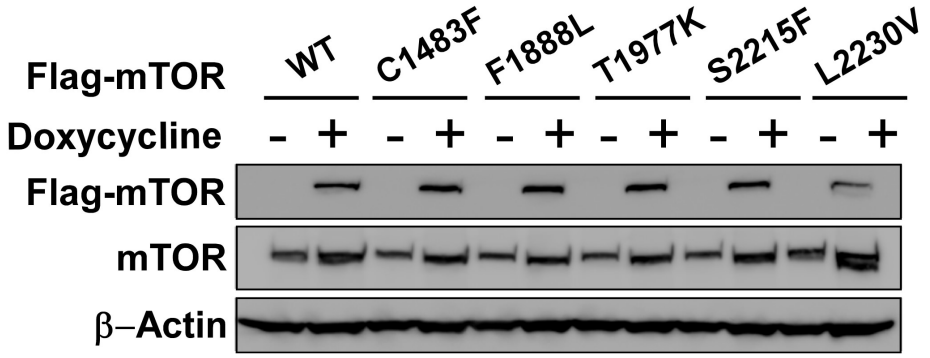

Supplementary Figure 6

Supplementary Figure 6 Tetracycline-inducible expression of mTOR in HeLa cells. HeLa cells expressing the indicated tetracycline-inducible WT or mutant mTOR were treated with doxycycline for 2 days and subjected to immunoblot analysis using the indicated antibodies.

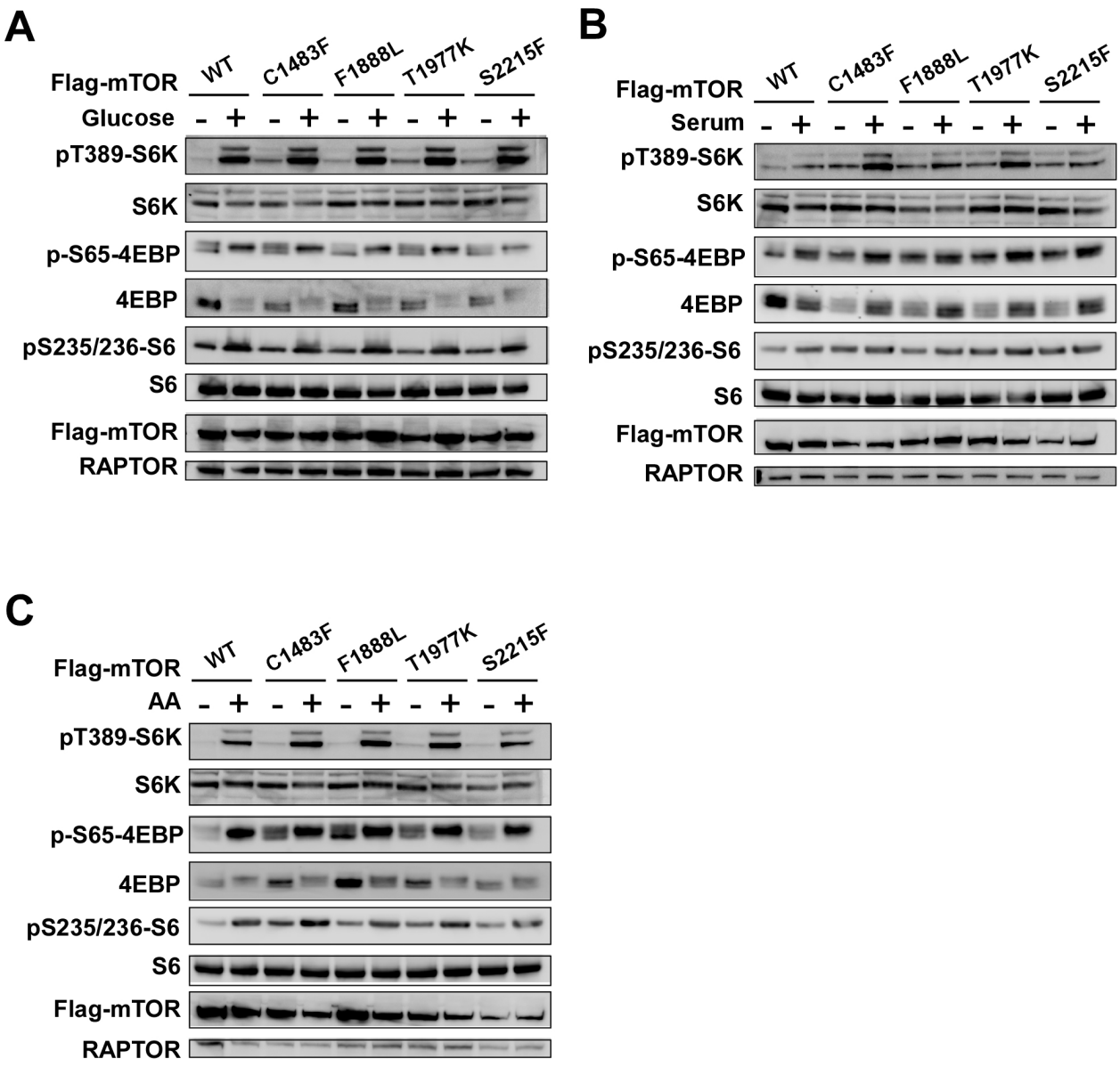

Supplementary Figure 7

Supplementary Figure 7 Characterization of nutrient dependence of mTORC1 signaling conferred by mTOR activating mutations. (A-C) Tetracycline-inducible HeLa cells expressing WT or mutant mTOR were either starved for glucose (**A**) or serum (**B**), or amino acids (**C**) for 1 hour, or starved for 1 hour and restimulated with full media for 1 hour, and subsequently subjected to immunoblot analysis using the indicated antibodies.

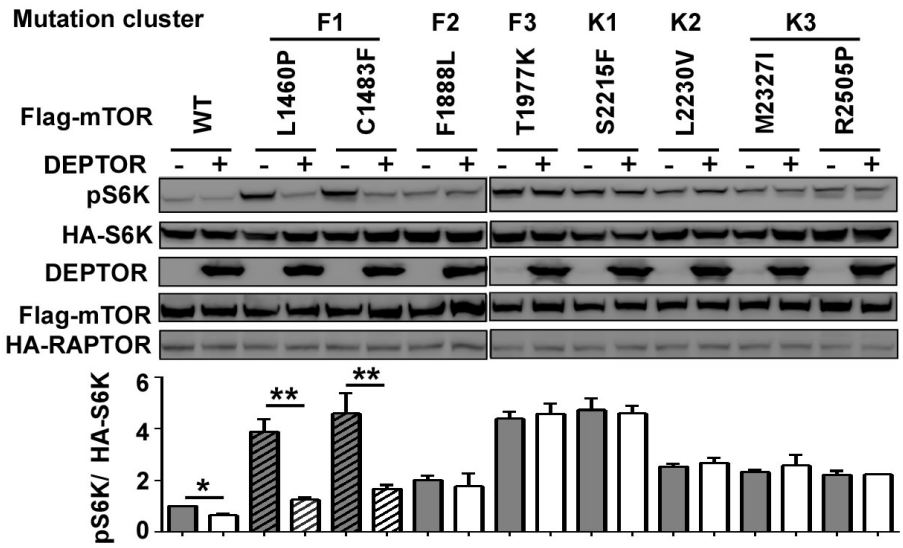

Supplementary Figure 8

Supplementary Figure 8 Characterization of the response of mTOR activating mutants to DEPTOR-mediated inhibition. 293T cells, transfected with vectors expressing HA-S6K, the indicated Flag-mTOR mutants, and either GFP or non-degradable DEPTOR, were subjected to immunoblot analysis using the indicated antibodies. Densitometry of phosphorylated S6K (T389) versus HA-S6K from three independent experiments is shown (mean ± SEM, n = 3 independent experiments). *, $P < 0.05$; **, $P < 0.01$ (*t*-test). The hatched bars indicate the mutants with significant inhibition by DEPTOR.

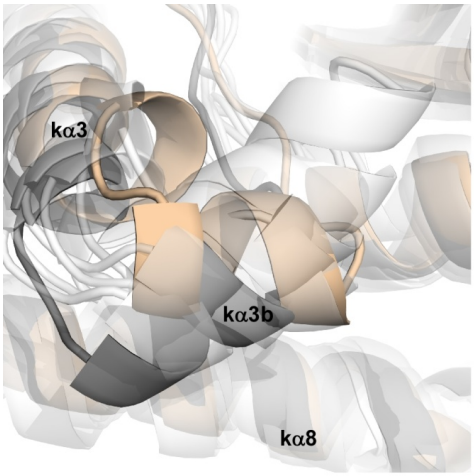

Supplementary Figure 9

Supplementary Figure 9 mTOR S2215F mutation can cause conformational reorganization in the vicinity of the mutation. Superposition of helix kα3b and kα8 of WT(gray), S2215F trajectory that is highlighted in the main text (wheat), and another eight S2215F trajectories (ghosted white) of mTOR kinase domain, at 501 ns of simulation. Of note, 5 simulation trajectories break away from the WT conformation after 100 ns of simulation, while 4 do not. One of the 10 simulations was only 471 nanoseconds. This trajectory is not shown above, but it should be noted that it was in the wild type conformation at 471 ns.

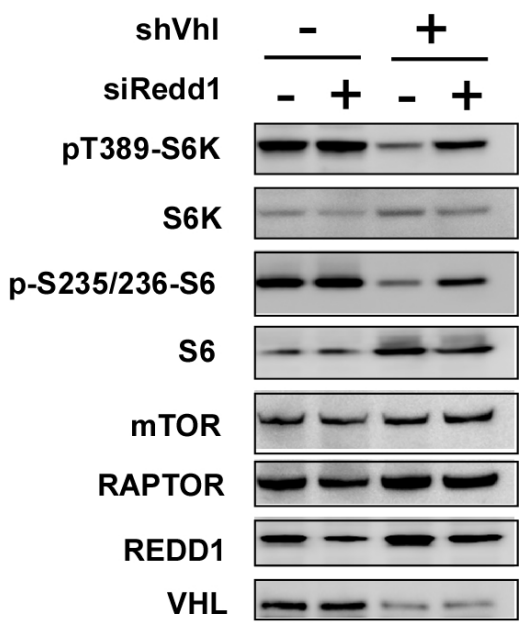

Supplementary Figure 10

Supplementary Figure 10 REDD1 is a major factor in regulating mTOR downstream of VHL loss. NIH/3T3 cells stably expressing shRNA against luciferase or Vhl were transient transfected with siRNA targeting scramble sequence or Redd1. 48 hours post transfection, cells were harvested and whole cell lysates were subjected to immunoblot analysis using the indicated antibodies.

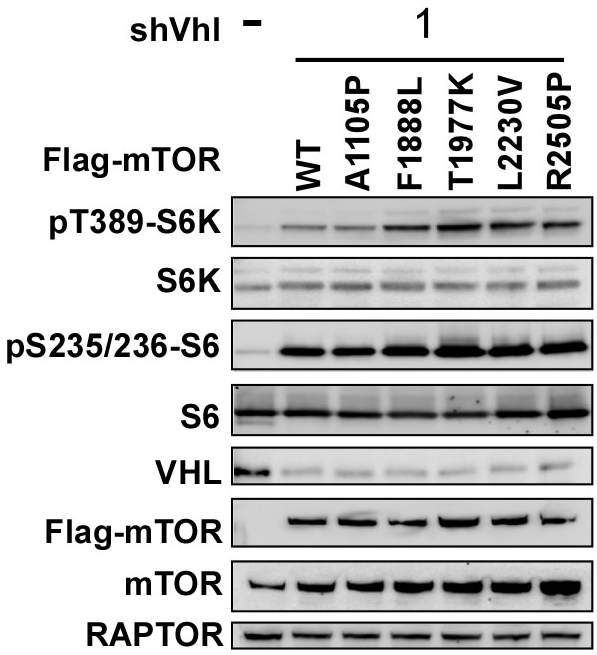

Supplementary Figure 11

Supplementary Figure 11 Expression of mTOR and shRNA against Vhl in NIH/3T3 cells. NIH/3T3 cells stably expressing shRNA against luciferase or Vhl as well as the indicated WT or mutant mTOR (A1105P, F1888L, T1977K, L2230V, and R2505P) were starved for serum for 1 hour and restimulated with full media for 1 hour before subjected to immunoblot analysis using the indicated antibodies.

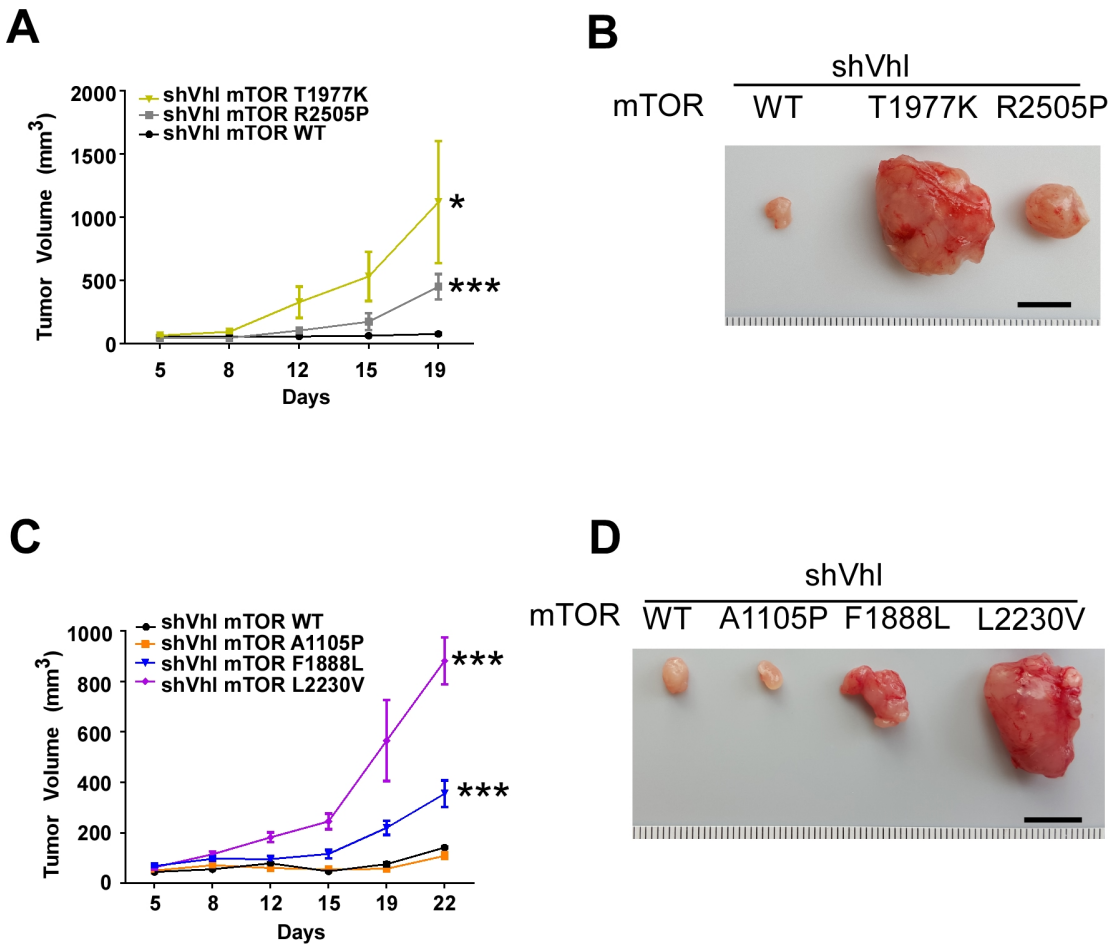

Supplementary Figure 12

Supplementary Figure 12 Kidney cancer-derived mTOR activating mutants can promote tumor growth *in vivo*. (A,C) NIH/3T3 cells expressing shVhl alone or NIH/3T3 cells expressing shVhl and the indicated WT or mutant mTOR (A1105P, F1888L, T1977K, L2230V, and R2505P) were implanted subcutaneously into the flanks of 6-8 weeks-old female NSG mice. Tumor size was measured for 19-22 days. The error bars represent SEM. *, $P < 0.05$, ***, $P < 0.001$ (two way ANOVA), n=4. **(B,D)** Images of harvested tumors or implanted tissues at day 22 or 19. Scale bar= 1 cm.

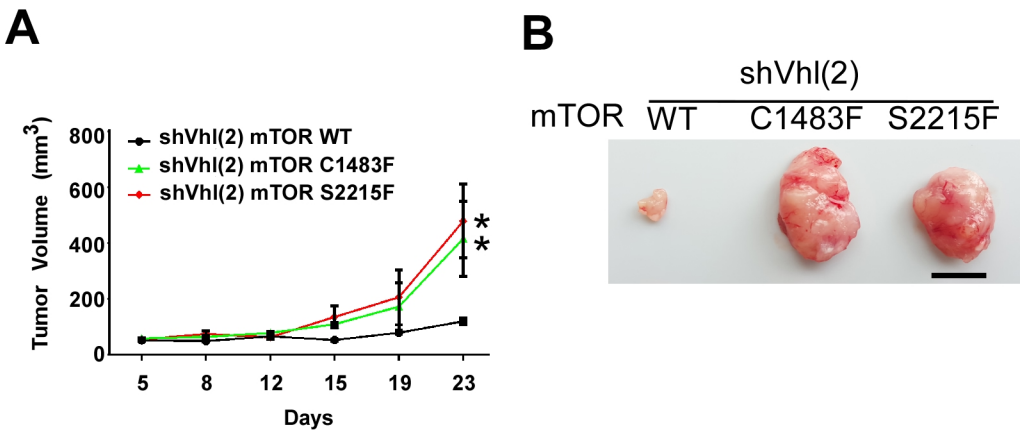

Supplementary Figure 13

Supplementary Figure 13 Kidney cancer-derived mTOR activating mutants can promote tumor growth *in vivo*. (A) NIH/3T3 cells expressing shVhl (second construct) and the indicated WT or mutant mTOR (C1483F, and S2215F) were implanted subcutaneously into the flanks of 6-8 weeks-old female NSG mice. Tumor size was measured for 23 days. The error bars represent SEM. *, $P < 0.05$ (two way ANOVA), n=4. **(B)** Images of harvested tumors or implanted tissues at day 23. Scale bar= 1 cm.

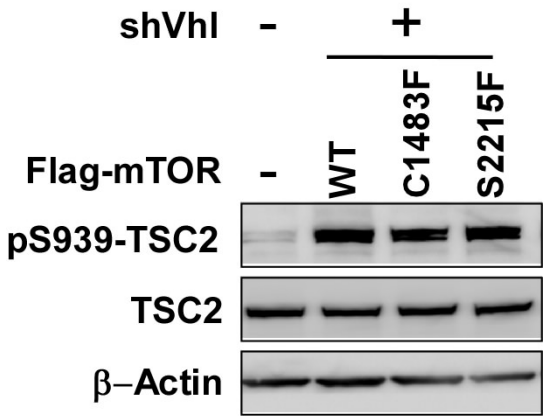

Supplementary Figure 14

Supplementary Figure 14 TSC2 is phosphorylated in shVhl NIH/3T3 cells expressing WT or mutant mTOR. NIH/3T3 cells treated with 1nM GDC0941 for 1 hour (first lane, for negative control), or shVhl NIH/3T3 cells expressing the indicated WT or mutant mTOR (C1483F, and S2215F) starved for serum for 1 hour and restimulated with full media for 1 hour were subjected to immunoblot analysis using the indicated antibodies.

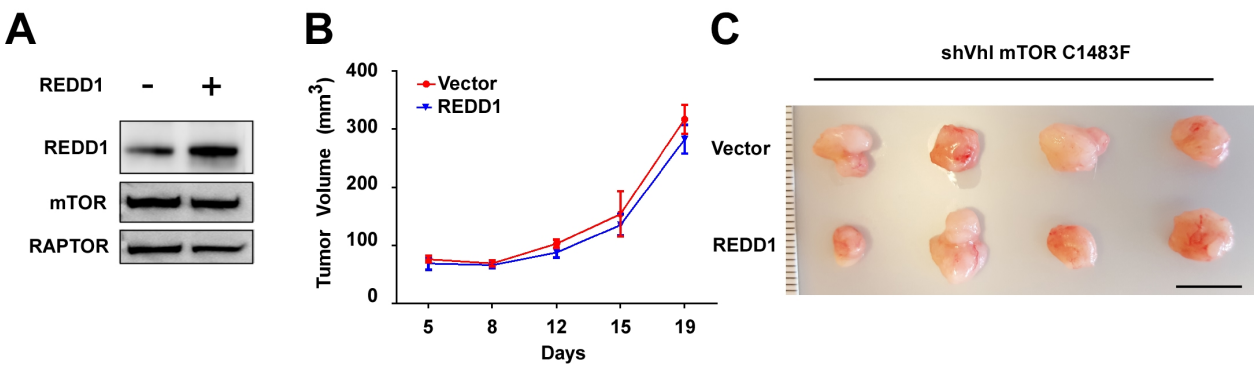

Supplementary Figure 15

Supplementary Figure 15 Tumors formed by NIH/3T3 cells expressing shVhl and mutant mTOR are resistant to REDD1-mediated inhibition in vivo. (A) NIH/3T3 cells stably expressing shVhl, mTOR mutant (C1483F), vector control or REDD1 were subjected to immunoblot analysis using the indicated antibodies. **(B)** NIH/3T3 cells expressing shVhl, mutant mTOR (C1483F) and vector or REDD1 were implanted subcutaneously into the flanks of 6-8 weeks-old female NSG mice. Tumor sizes were measured up to 19 days. Error bars represent SEM, n=4. **(C)** Images of harvested tumors or implanted tissues at day 19. Scale bar= 1 cm.

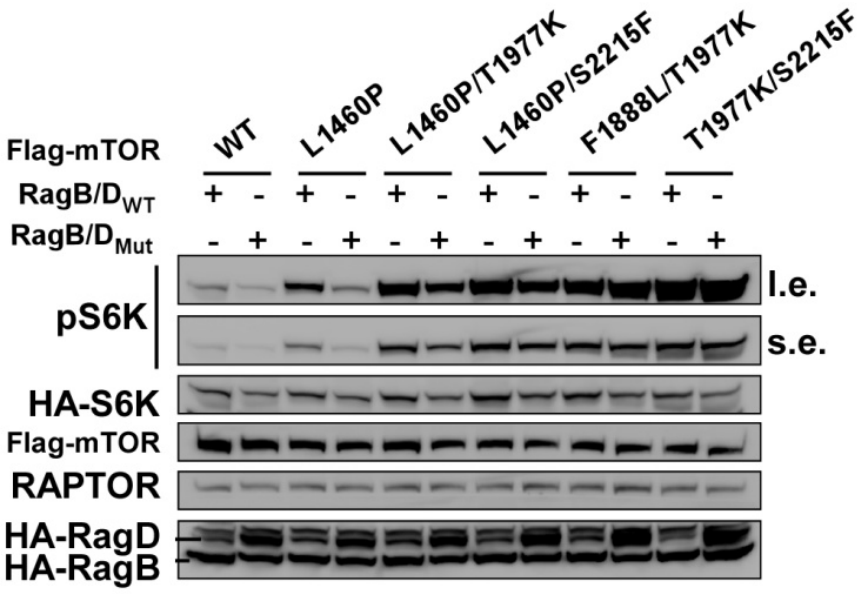

Supplementary Figure 16

Supplementary Figure 16 The mTOR double mutations confer resistance to dominant-negative Rag GTPase. 293T cells were transfected with vector expressing HA-S6K, the indicated Flag-mTOR mutants, and either RagB plus RagD (RagB/D_{WT}) or dominant negative $RagB^{GDP}$ plus $RagD^{GTP}$ (RagB/D_{Mut}). Whole cell lysates were subjected to immunoblot analysis using the indicated antibodies. l.e, long exposure; s.e, short exposure.

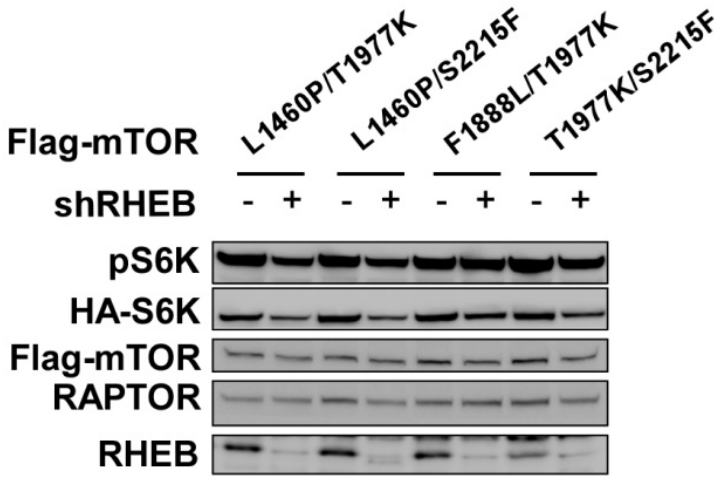

Supplementary Figure 17

Supplementary Figure 17 The mTOR double mutants are not dependent on RHEB for mTORC1 signaling. HeLa cells stably expressing shRNA against GFP or RHEB were transfected with vectors expressing HA-S6K and the indicated Flag-mTOR mutants, and analyzed by the indicated immunoblots.

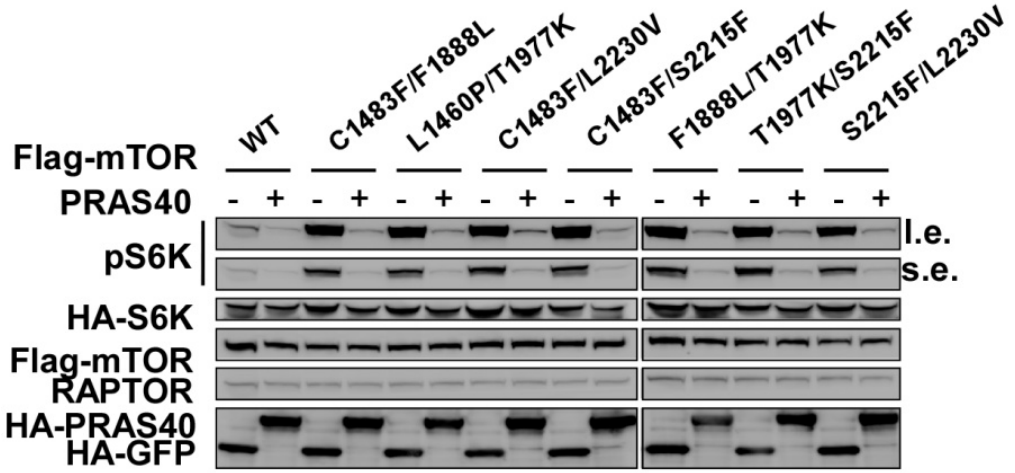

Supplementary Figure 18

Supplementary Figure 18 The mTOR double mutants are sensitive to PRAS40-mediated inhibition. 293T cells were transfected with vectors expressing HA-S6K, the indicated Flag-mTOR mutants and either GFP or PRAS40. Whole cell lysates were subjected to immunoblot analysis using the indicated antibodies. l.e, long exposure; s.e, short exposure.

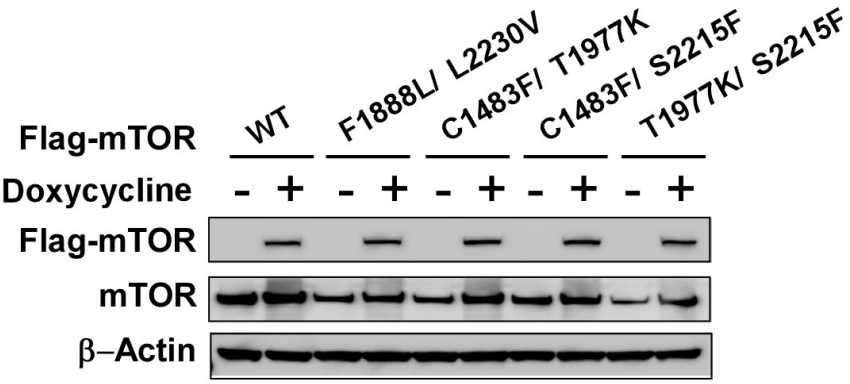

Supplementary Figure 19

Supplementary Figure 19 Tetracycline-inducible expression of mTOR in HeLa cells. HeLa cells expressing the indicated tetracycline-inducible WT or double mutant mTOR were treated with doxycycline for 2 days and subjected to immunoblot analysis using the indicated antibodies.

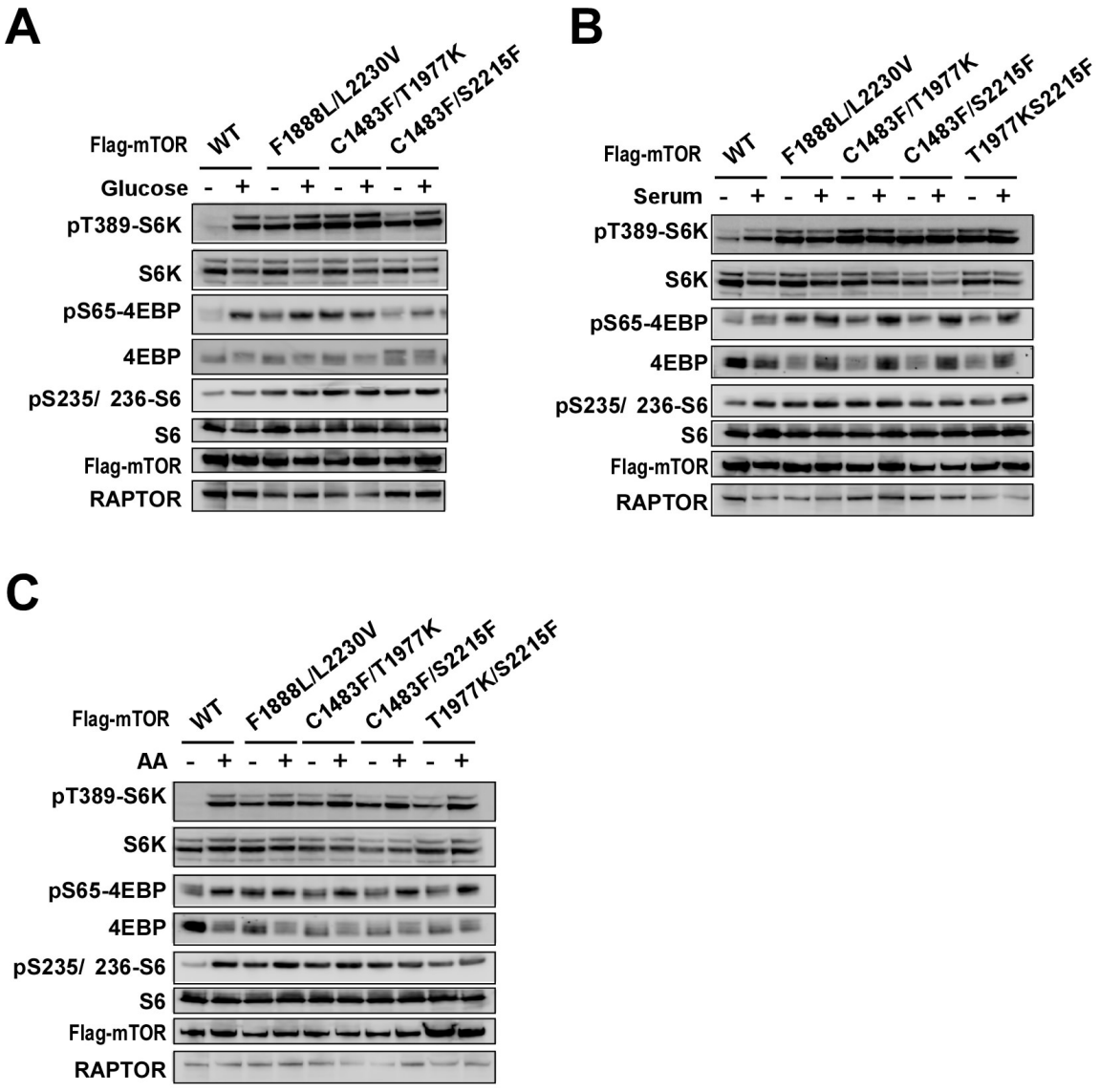

Supplementary Figure 20

Supplementary Figure 20 Characterization of nutrient dependence of mTORC1 signaling conferred by mTOR double mutations. (A-C) HeLa cells expressing tetracycline-inducible WT or mutant mTOR were treated with doxycycline for 48 hours to induce mTOR. Cells were then starved for glucose (**A**), serum (**B**) or amino acids (**C**) for 1 hour, or starved for 1 hour and restimulated with full media for 1 hour, and subjected to immunoblot analysis using the indicated antibodies.

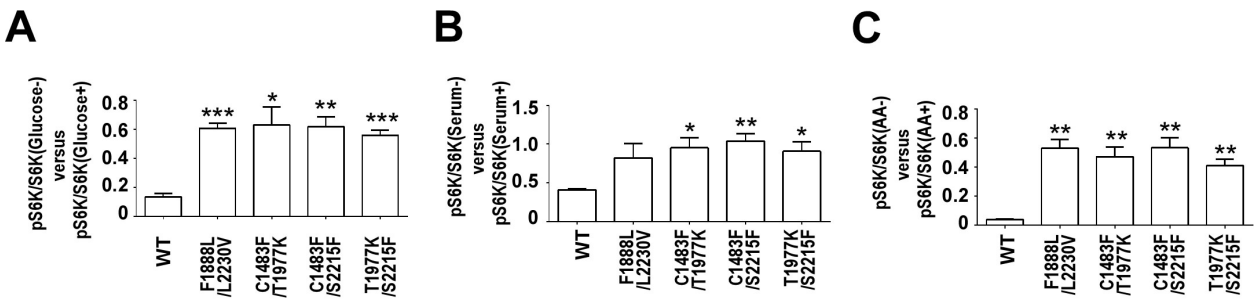

Supplementary Figure 21

Supplementary Figure 21 Quantification of mTORC1 signaling of mTOR double mutations upon various nutrient deprivation versus restimulation condition. (A) Ratio of densitometry of pS6K/HA-S6K (glucose deprivation) versus pS6K/HA-S6K (glucose restimulation). **(B)** Ratio of densitometry of pS6K/HA-S6K (Serum deprivation) versus pS6K/HA-S6K (Serum restimulation). **(C)** Ratio of densitometry of pS6K/HA-S6K (amino acid deprivation) versus pS6K/HA-S6K (amino acid restimulation). Densitometry signals are from Figure 9 A-C. For all the panels, *, $P < 0.05$; **, $P < 0.01$; ***, $P < 0.001$ (*t*-test, comparison between indicated mutants and WT).

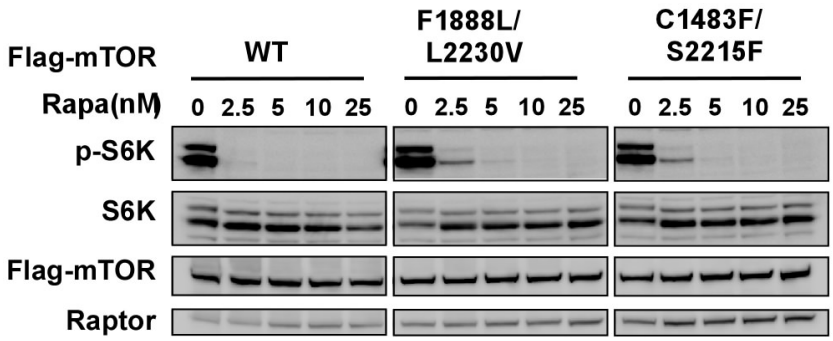

Supplementary Figure 22

Supplementary Figure 22 Characterization of sensitivity to rapamycin of mTOR double mutations. Tetracycline-inducible HeLa cells expressing WT or mutant mTOR were treated with the indicated doses of rapamycin for 1 hour prior to the immunoblot analysis using the indicated antibodies.

Supplementary Table 1. List of mTOR missense mutations from TCGA, COSMIC, Novartis, other publications, and current study.

AA position	AA change	cDNA change*	Domain	Cancer relavance	ID / resources	Reference
5	G -> R		HEAT	Kidney-ccRCC	TCGA-AK-3429-01	
8	A -> S		HEAT	Lung		PMID: 20190810
9	A -> T		HEAT	Breast	TCGA-A8-A08S-01	
21	V -> I		HEAT	Colorectal	TCGA-A6-6781-01	
30	K -> N		HEAT	Bladder	TCGA-FD-A6TA-01	
41	A -> P		HEAT	CCLE	NCIH650_LUNG	PMID: 24631838
41	A -> T		HEAT	CCLE	SKUT1_SOFT_TISSUE	PMID: 24631838
41	A -> S		HEAT	Ovary	TCGA-25-1329-01	PMID: 24631838
42	K -> M		HEAT	COSMIC	COSMIC	
53	R -> Q		HEAT	Colorectal	TCGA-AA-3877-01	
55	M -> I		HEAT	Head & neck	TCGA-HL-7533-01	
58	E -> Q		HEAT	Breast	Novartis	
61	T -> A		HEAT	Pancreas	Novartis	
68	N -> K		HEAT	Lung	TCGA-66-2765-01	
101	A -> V		HEAT	Melanoma	TCGA-GF-A6C9-06	
103	R -> Q		HEAT	Uterus	TCGA-AP-A059-01	
124	E -> D		HEAT	Uterus	TCGA-B5-A0JY-01	
125	M -> I		HEAT	Esophagus	ESCC-D16	
133	L -> V		HEAT	Breast	TCGA-BH-A0DZ-01	
135	M -> T		HEAT	COSMIC	COSMIC	PMID: 20190810
135	M -> V		HEAT	Liver	TCGA-G3-A5SJ-01	
140	F -> L		HEAT	CCLE	NCIH2066_LUNG	
161	N -> S		HEAT	COSMIC	COSMIC	
163	G -> S		HEAT	Stomach	Novartis	
173	R -> C		HEAT	Liver	H112345	
178	S -> N		HEAT	COSMIC	COSMIC	
180	P -> S		HEAT	Melanoma	TCGA-EE-A29G-06	
188	Q -> R		HEAT	COSMIC	COSMIC	
194	I -> V		HEAT	Uterus	TCGA-D1-A17Q-01	
199	W -> L		HEAT	Lung	LUAD-S01478	
203	Q -> H		HEAT	Lung	LUAD-B00523	
204	A -> T		HEAT	Melanoma	YUKLAB	
211	A -> V		HEAT	Esophagus	ESO-859	
237	T -> A		HEAT	CCLE	SNU410_PANCREAS	

241	A -> S		HEAT	COSMIC	COSMIC	
243	K -> R		HEAT	CCLE	REH_HAEMATOPOIET	
250	A -> V		HEAT	Colorectal	TCGA-AA-3663-01	
256	N -> S		HEAT	Breast	TCGA-BH-A0E6-01	
260	R -> Q		HEAT	Esophagus	TCGA-VQ-A8P2-01	
261	I -> V		HEAT	CCLE	2313287_STOMACH	
262	H -> R		HEAT	CCLE	2313287_STOMACH	
267	I -> V		HEAT	Stomach	TCGA-BR-6452-01	
270	E -> K		HEAT	Stomach	TCGA-HU-A4GX-01	
270	E -> K		HEAT	Uterus	TCGA-B5-A0JY-01	
275	S -> T		HEAT	CCLE	KCL22_HAEMATOPOI	
281	R -> C		HEAT	NCI60	HCC_2998	
281	R -> H		HEAT	Ovary	TCGA-61-1733-01	
281	R -> C		HEAT	Stomach	TCGA-BR-4184-01	
291	Q -> L		HEAT	COSMIC	COSMIC	
293	Q -> K		HEAT	COSMIC	COSMIC	
298	K -> E		HEAT	COSMIC	COSMIC	
304	M -> I		HEAT	Lung	TCGA-44-6145-01	
311	R -> C		HEAT	Stomach	TCGA-BR-8382-01	
314	T -> N		HEAT	COSMIC	COSMIC	
336	Y -> C		HEAT	Stomach	TCGA-CG-5723-01	
342	L -> P		HEAT	CCLE	CCK81_LARGE_INTE	
370	F -> Y		HEAT	Ovary	TCGA-23-1122-01	
373	V -> L		HEAT	Kidney-nccRCC	TCGA-BQ-7061-01	
382	N -> S		HEAT	Breast	Novartis	
384	K -> R		HEAT	Stomach	TCGA-CG-4442-01	
384	K -> N		HEAT	Uterus	TCGA-BS-A0UV-01	
385	N -> I		HEAT	Melanoma	TCGA-D3-A2JH-06	
386	S -> W		HEAT	COSMIC	COSMIC	
398	R -> C		HEAT	Lung	631056	
403	R -> Q		HEAT	Colorectal	587222	
410	T -> N		HEAT	Breast	TCGA-A7-A26J-01	
416	T -> A		HEAT	Stomach	TCGA-BR-A4QL-01	
420	V -> I		HEAT	CCLE	22RV1_PROSTATE	
431	T -> A		HEAT	CCLE	SNU1_STOMACH	
432	A -> V		HEAT	Breast	Novartis	
432	A -> V		HEAT	Liver	Novartis	
438	G -> W		HEAT	COSMIC	COSMIC	
440	L -> F		HEAT	Lung	LUAD-NYU284	
443	A -> T		HEAT	Breast	Novartis	
447	E -> Q		HEAT	Cervix	TCGA-JW-A5VL-01	

453	P -> L		HEAT	CCLE	COLO792_SKIN	
469	A -> T		HEAT	Colorectal	TCGA-AA-3715-01	
471	K -> T		HEAT	Stomach	TCGA-BR-8589-01	
475	A -> G		HEAT	Breast	TCGA-A8-A09B-01	
476	M -> V		HEAT	Breast	Novartis	
477	Q -> H		HEAT	Stomach	TCGA-F1-6177-01	
480	A -> T		HEAT	Uterus	TCGA-B5-A11E-01	
488	M -> I		HEAT	CCLE	CW2_LARGE_INTEST	
491	R -> Q		HEAT	Colorectal	587246	
492	A -> T		HEAT	Brain/CNS	TCGA-02-0083-01	
523	D -> Y		HEAT	COSMIC	COSMIC	
536	Q -> P		HEAT	Lung	TCGA-69-7980-01	
537	D -> N		HEAT	COSMIC	COSMIC	
545	L -> M		HEAT	Esophagus	TCGA-L5-A4OH-01	
547	L -> F		HEAT	Melanoma	TCGA-D3-A2JF-06	
551	P -> L		HEAT	Melanoma	TCGA-EE-A20B-06	
551	P -> L		HEAT	Melanoma	TCGA-IH-A3EA-01	
553	R -> H		HEAT	COSMIC	COSMIC	
570	L -> F		HEAT	Melanoma	TCGA-EE-A2A5-06	
571	T -> K		HEAT	CCLE	MOLM13_HAEMATOPO	
571	T -> M		HEAT	Colorectal	TCGA-AA-3854-01	
571	T -> M		HEAT	Stomach	Novartis	
573	L -> F		HEAT	CCLE	KYM1_SOFT_TISSUE	
578	D -> Y		HEAT	COSMIC	COSMIC	
588	T -> M		HEAT	CCLE	SNU175_LARGE_INT	
598	S -> F		HEAT	Melanoma	YULAN	
602	F -> L		HEAT	Head & neck	TCGA-CV-6933-01	
604	R -> C		HEAT	Stomach	TCGA-BR-8680-01	
604	R -> H		HEAT	Uterus	TCGA-AP-A0LM-01	
607	A -> V		HEAT	Lung	TCGA-22-5473-01	
610	F -> V		HEAT	Stomach	TCGA-BR-8589-01	
622	A -> D		HEAT	COSMIC	COSMIC	
623	A -> T		HEAT	COSMIC	COSMIC	
624	R -> H		HEAT	Bladder	DS-bla-018	
624	R -> H		HEAT	Uterus	TCGA-AP-A0LM-01	
628	R -> H		HEAT	Colorectal	587342	
637	I -> V		HEAT	Breast	Novartis	
639	G -> D		HEAT	Lung	LUAD-S01405	
640	H -> R		HEAT	Breast	Novartis	
642	H -> Y		HEAT	Melanoma	TCGA-EB-A431-01	
645	S -> C		HEAT	CCLE	NCIH1568_LUNG	

647	T -> I		HEAT	CCLE	OVK18_OVARY	
648	A -> T		HEAT	Colorectal	TCGA-AA-3821-01	
668	D -> Y		HEAT	Lung	TCGA-69-7980-01	
670	D -> H		HEAT	Liver	TCGA-CC-A5UC-01	
672	R -> C		HEAT	Melanoma	TCGA-ER-A19F-06	
681	E -> D		HEAT	Stomach	Novartis	
691	E -> D		HEAT	CCLE	HCC1171_LUNG	
695	A -> V		HEAT	CCLE	HT115_LARGE_INTE	
695	A -> S		HEAT	COSMIC	COSMIC	
695	A -> D		HEAT	COSMIC	COSMIC	
696	L -> F		HEAT	Colorectal	TCGA-A6-6651-01	
699	A -> P		HEAT	Lung	TCGA-37-4135-01	
704	V -> M		HEAT	CCLE	HEC6_ENDOMETRIUM	
706	E -> Q		HEAT	Lung	TCGA-49-4486-01	
709	E -> G		HEAT	Head & neck	TCGA-CV-5966-01	
716	G -> S		HEAT	Colorectal	587336	
716	G -> D		HEAT	Lung	TCGA-91-6829-01	
717	R -> Q		HEAT	Bladder	TCGA-BT-A20R-01	
717	R -> L	2150G>T	HEAT	Kidney-ccRCC	Novartis RECORD-3	
717	R -> L		HEAT	Lung	585270	
720	S -> I		HEAT	Lung	LUAD-5V8LT	
722	N -> D		HEAT	Stomach	TCGA-BR-8487-01	
735	I -> S		HEAT	Lung	TCGA-18-3421-01	
735	I -> N		HEAT	Stomach	pfg008T	
738	L -> F		HEAT	Breast	TCGA-E9-A228-01	
745	G -> W		HEAT	Prostate	TCGA-HC-7081-01	
754	A -> G		HEAT	Ovary	TCGA-29-1691-01	
755	R -> H		HEAT	COSMIC	COSMIC	
755	R -> L		HEAT	Lymph	M025	
773	E -> D		HEAT	Uterus	TCGA-AP-A051-01	
783	L -> R		HEAT	Colorectal	587376	
789	D -> V		HEAT	Colorectal	TCGA-AA-3867-01	
822	I -> V		HEAT	Esophagus	TCGA-LN-A4A5-01	
825	M -> I		HEAT	CCLE	KCL22_HAEMATOPOI	
835	A -> T		HEAT	COSMIC	COSMIC	
835	A -> S		HEAT	Uterus	TCGA-AP-A059-01	
838	Q -> L		HEAT	COSMIC	COSMIC	
844	L -> M		HEAT	Esophagus	TCGA-L5-A891-01	
858	Y -> C		HEAT	COSMIC	COSMIC	
860	K -> N		HEAT	Kidney-ccRCC	TCGA-B0-5119-01	Current study
861	Y -> H		HEAT	CCLE	EN_ENDOMETRIUM	

866	E -> K		HEAT	Colorectal	TCGA-AA-3956-01	
875	E -> K		HEAT	Ovary	TCGA-04-1338-01	
878	Q -> P		HEAT	Lung	TCGA-95-7567-01	
881	R -> C		HEAT	Stomach	TCGA-BR-8487-01	
886	R -> C		HEAT	Stomach	pfg008T	
888	L -> F		HEAT	COSMIC	COSMIC	
891	L -> V		HEAT	Uterus	TCGA-AX-A0J0-01	
904	G -> V		HEAT	Liver	H060638	
910	R -> Q		HEAT	Stomach	TCGA-HU-A4GQ-01	
911	D -> Y		HEAT	Lung	LUAD-NYU1051S	
915	V -> F		HEAT	Esophagus	TCGA-RD-A8MV-01	
919	E -> V		HEAT	Kidney-ccRCC		Current study PMID: 24622468
928	D -> N		HEAT	Melanoma	TCGA-D3-A51N-06	
929	Y -> C		HEAT	Breast	Novartis	
933	E -> K		HEAT	Esophagus	TCGA-LN-A49M-01	
957	R -> Q		HEAT	Stomach	TCGA-BR-8361-01	
968	H -> Y		HEAT	COSMIC	COSMIC	
981	S -> F		HEAT	Melanoma	MEL-JWCI-WGS-22	
1002	R -> Q		HEAT	Esophagus	ESCC-233T	
1009	R -> L		HEAT	Lung	TCGA-18-3414-01	
1009	R -> L		HEAT	Melanoma	ME050	
1022	F -> S		HEAT	Uterus	TCGA-BG-A0M4-01	
1033	E -> K		HEAT	CCLE	VMCUB1_URINARY_T	
1036	T -> N		HEAT	Colorectal	TCGA-CM-4752-01	
1044	M -> I		HEAT	Lung	TCGA-91-6840-01	
1048	I -> L		HEAT	Breast	TCGA-AN-A046-01	
1063	L -> F		HEAT	Colorectal	TCGA-AA-3984-01	
1066	E -> D		HEAT	Uterus	TCGA-D1-A0ZO-01	
1067	F -> V		HEAT	Stomach	pfg062T	
1078	M -> I		HEAT	Colorectal	TCGA-G4-6320-01	
1080	R -> P		HEAT	Cervix	TCGA-EA-A556-01	
1080	R -> C		HEAT	Colorectal	TCGA-G4-6298-01	
1083	M -> V		HEAT	Breast	Novartis	
1087	S -> N		HEAT	CCLE	SNU1040_LARGE_IN	
1103	F -> Y		HEAT	Ovary	TCGA-04-1525-01	
1105	A -> P		HEAT	Kidney-ccRCC	TCGA-CJ-4887	Current study
1105	A -> T		HEAT	Melanoma	TCGA-ER-A2NF-01	
1105	A -> T		HEAT	Melanoma	TCGA-ER-A2NF-06	
1105	A -> T		HEAT	Ovary	TCGA-24-2254-01	
1106	N -> K		HEAT	Ovary	TCGA-24-1556-01	
1117	P -> S		HEAT	Melanoma	YUBER	

1124	A -> V		HEAT	Uterus	TCGA-AP-A0LE-01	
1134	A -> V		HEAT	Breast	Novartis	
1134	A -> V		HEAT	CCLE	ABC1_LUNG	
1134	A -> V		HEAT	CCLE	MOTN1_HAEMATOPOI	
1134	A -> T		HEAT	NCI60	MOLT_4	
1134	A -> V		HEAT	Stomach	Novartis	
1141	R -> S		HEAT	Lung	TCGA-18-3416-01	
1145	S -> F		HEAT	Melanoma	MEL-JWCI-WGS-34	
1151	Y -> C		HEAT	CCLE	C2BBE1_LARGE_INT	
1151	Y -> C		HEAT	Lung	TCGA-38-4631-01	
1160	V -> G		HEAT	Uterus	TCGA-BK-A0C9-01	
1161	R -> Q		HEAT	CCLE	DMS454_LUNG	
1161	R -> Q		HEAT	Head & neck	HN_62469	
1164	D -> N		HEAT	Breast	Novartis	
1170	R -> H		HEAT	Esophagus	ESO-161	
1178	S -> F		HEAT	CCLE	J82_URINARY_TRACT	
1186	K -> E		HEAT	COSMIC	COSMIC	
1190	I -> L		HEAT	COSMIC	COSMIC	
1193	P -> L		HEAT	CCLE	COLO201_LARGE_IN	
1193	P -> L		HEAT	CCLE	COLO205_LARGE_IN	
1199	L -> M		HEAT	Pancreas	TCGA-IB-7651-01	
1201	R -> Q		HEAT	CCLE	AN3CA_ENDOMETRIUM	
1208	R -> C		HEAT	Breast	Novartis	
1208	R -> C		HEAT	CCLE	HEC59_ENDOMETRIUM	PMID: 24631838
1208	R -> C		HEAT	CCLE	KALS1_CENTRAL_NE	PMID: 24631838
1208	R -> C		HEAT	CCLE	KYSE510_OESOPHAGUS	PMID: 24631838
1213	I -> V		HEAT	COSMIC	COSMIC	
1215	R -> T		HEAT	Breast	TCGA-E2-A1IN-01	
1224	D -> Y		HEAT	Breast	Novartis	
1225	E -> K		HEAT	Pancreas	TCGA-HZ-8636-01	
1239	S -> N		HEAT	Uterus	TCGA-BG-A0MC-01	
1241	Q -> R		HEAT	Brain/CNS	Sample_16	
1244	A -> E		HEAT	Colorectal	TCGA-AA-3663-01	
1254	P -> T		HEAT	CCLE	KCL22_HAEMATOPOI	
1254	P -> L		HEAT	CCLE	KM12_LARGE_INTES	
1266	Q -> K		HEAT	Esophagus	TCGA-JY-A6F8-01	
1271	A -> T		HEAT	Lung	S00837	
1276	S -> F		HEAT	CCLE	HEC265_ENDOMETRIUM	
1280	W -> C		HEAT	Lung	TCGA-64-5781-01	

1301	R -> L		HEAT	Lung	LUAD-NYU160	
1303	C -> F		HEAT	Colorectal	TCGA-AA-3980-01	
1304	W -> R		HEAT	CCLE	KMRC20_KIDNEY	
1312	P -> L		HEAT	Colorectal	TCGA-AA-3710-01	
1313	M -> I		HEAT	COSMIC	COSMIC	
1313	M -> L		HEAT	Lung	LUAD-RT-S01699	
1315	R -> S		HEAT	CCLE	NCIH1930_LUNG	
1332	D -> N		HEAT	Uterus	TCGA-AP-A059-01	
1337	L -> I		HEAT	COSMIC	COSMIC	
1368	D -> N		FAT	Stomach	Novartis	
1378	N -> S		FAT	Liver	Novartis	
1395	K -> E		FAT	COSMIC	COSMIC	
1408	P -> S		FAT	CCLE	CW2_LARGE_INTEST	
1409	T -> P		FAT	Lung	LUAD-S01302	
1426	P -> L		FAT	Colorectal	TCGA-AZ-6601-01	
1427	E -> Q		FAT	CCLE	MDAMB361_BREAST	
1428	A -> T		FAT	COSMIC	COSMIC	PMID: 24631838
1428	A -> V		FAT	COSMIC	COSMIC	
1430	A -> V		FAT	Uterus	TCGA-B5-A11E-01	PMID: 17360675
1431	G -> R		FAT	Colorectal	EV-026-P	
1431	G -> R		FAT	Colorectal	TCGA-G4-6309-01	
1433	L -> S		FAT	Breast	SA237	PMID: 24631838
1433	L -> S		FAT	Kidney-ccRCC	TCGA-BP-5001-01	Current study, PMID: 24631838,
1433	L -> S		FAT	Kidney-nccRCC	9266920	PMID: 24631838
1452	K -> N		FAT	Kidney-ccRCC	TCGA-CZ-5987-01	PMID: 24631838
1456	W -> R		FAT	CCLE	NALM6_HAEMATOPOI	
1459	A -> D	4376C>A	FAT	Kidney-ccRCC	Novartis RECORD-3	
1459	A -> P		FAT	Kidney-ccRCC	TCGA-BP-5176-01	Current study, PMID: 24631838, 17360675
1460	L -> P		FAT	Kidney-ccRCC	TCGA-B0-5701-01	Current study
1460	L -> P		FAT	Kidney-ccRCC	TCGA-BP-5175-01	Current study
1461	V -> A		FAT	Breast	Novartis	
1461	V -> L		FAT	Ovary	TCGA-61-1907-01	
1463	Y -> S		FAT	Kidney-ccRCC	TCGA-B0-5697-01	PMID: 24631838
1465	K -> N		FAT	COSMIC	COSMIC	
1467	M -> I		FAT	Cervix	TCGA-DG-A2KM-01	
1473	D -> H		FAT	Bladder	B25	
1480	R -> H		FAT	Colorectal	TCGA-AU-6004-01	
1482	R -> H		FAT	Breast	Novartis	
1482	R -> C		FAT	Breast	Novartis	

1482	R -> C		FAT	CCLE	MFE296_ENDOMETRIUM	
1482	R -> C		FAT	Stomach	TCGA-HJ-7597-01	
1483	C -> R		FAT	Brain/CNS		PMID: 24631838
1483	C -> W		FAT	Breast	BR-M-059	PMID: 24631838
1483	C -> Y		FAT	CCLE	MOLT16_HAEMATOPO	PMID: 24631838
1483	C -> F		FAT	Kidney-ccRCC		Current study, PMID: 24631838, 17360675
1483	C -> Y		FAT	Kidney-ccRCC	TCGA-B0-5696-01	
1485	E->K		FAT			PMID: 24631838
1491	G -> S		FAT	CCLE	EM2_HAEMATOPOIET	
1492	Q -> R		FAT	Breast	Novartis	
1494	H -> R		FAT	CCLE	HEC265_ENDOMETRIUM	
1497	C -> F		FAT	NCI60	HCC_2998	
1502	T -> A		FAT	Prostate	TCGA-HC-A48F-01	
1513	A -> T		FAT	Uterus	TCGA-D1-A17F-01	
1514	R -> Q		FAT	Lymph	DLBCL-MAYO_DLBCL	
1517	A -> V		FAT	Breast	TCGA-D8-A1J8-01	
1519	A -> T		FAT	Kidney-ccRCC	TCGA-CJ-6027-01	PMID: 24631838
1524	G -> V		FAT	Head & neck	TCGA-CR-7388-01	
1544	A -> T		FAT	Esophagus	TCGA-JY-A6FH-01	
1565	D -> H		FAT	Bladder	B104-0	
1567	A -> T		FAT	Esophagus	ESO-859	
1577	A -> V		FAT	COSMIC	COSMIC	PMID: 17360675
1590	M -> I		FAT	Stomach	TCGA-BR-4267-01	
1592	S -> Y		FAT	Uterus	TCGA-BS-A0UV-01	
1595	M -> V		FAT	Liver	TCGA-DD-A1EF-01	
1600	E -> A		FAT	Esophagus	ESO-859	
1612	R -> P		FAT	Breast	TCGA-BH-A0EE-01	
1612	R -> Q		FAT	CCLE	C32_SKIN	
1616	R -> H		FAT	Colorectal	TCGA-AA-3949-01	
1616	R -> C		FAT	Melanoma	TCGA-FW-A3R5-06	
1616	R -> H		FAT	Stomach	TCGA-HU-A4GX-01	
1624	Q -> R		FAT	Esophagus	TCGA-D7-A6EY-01	
1624	Q -> H		FAT	Esophagus	TCGA-L5-A4OI-01	
1635	K -> T		FAT	Uterus	TCGA-B5-A11N-01	
1640	R -> L		FAT	Lung	TCGA-66-2734-01	
1640	R -> W		FAT	Melanoma	YUKLAB	
1641	S -> F		FAT	Melanoma	TCGA-D3-A2JL-06	
1641	S -> F		FAT	Melanoma	TCGA-DA-A1HV-06	

1650	M -> V		FAT	Liver	H050566	
1652	T -> A		FAT	Kidney-ccRCC		PMID: 25159823
1655	K -> N		FAT	COSMIC	COSMIC	
1662	K -> M		FAT	Kidney-ccRCC	K251	PMID:22138691
1684	Q -> P		FAT	Prostate	PR-7520	
1692	V -> A		FAT	CCLE	BICR18_UPPER_AER	
1703	N -> S		FAT	Pancreas	TCGA-IB-7651-01	
1705	W -> R		FAT	COSMIC	COSMIC	
1708	A -> V		FAT	Uterus	TCGA-N6-A4V9-01	
1709	R -> H		FAT	CCLE	KYSE410_OESOPHAGUS	
1709	R -> H		FAT	Uterus	TCGA-B5-A11E-01	
1728	A -> S		FAT	CCLE	NCIH650_LUNG	
1728	A -> S		FAT	Lung	TCGA-95-7039-01	
1747	M -> L		FAT	COSMIC	COSMIC	
1749	R -> Q		FAT	CCLE	22RV1_PROSTATE	
1759	L -> R		FAT	Breast	TCGA-BH-A0AZ-01	
1762	Q -> H		FAT	COSMIC	COSMIC	
1763	G -> C		FAT	COSMIC	COSMIC	
1765	N -> D		FAT	CCLE	HT_HAEMATOPOIETI	
1769	I -> V		FAT	Esophagus	ESO-049	
1778	A -> S		FAT	Head & neck	NPC30F	
1783	D -> N		FAT	COSMIC	COSMIC	
1784	R -> H		FAT	Uterus	TCGA-AP-A0LM-01	
1792	A -> V		FAT	Colorectal	587238	
1792	A -> V		FAT	Colorectal	TCGA-F4-6570-01	
1799	E -> K		FAT	Blood	MM-0473	
1799	E -> K		FAT	Brain/CNS	TCGA-19-1790-01	
1799	E -> K		FAT	CCLE	HEC59_ENDOMETRIUM	
1799	E -> K		FAT	CCLE	HS683_CENTRAL_NE	
1799	E -> K		FAT	CCLE	SNU349_KIDNEY	
1799	E -> K		FAT	Cervix	TCGA-EX-A449-01	
1799	E -> K		FAT	Colorectal	EV-075-P	
1799	E -> K		FAT	Colorectal	TCGA-AA-3555-01	
1799	E -> K		FAT	Prostate	PR-00-1165	
1799	E -> K		FAT	Uterus	TCGA-AX-A0J0-01	
1799	E -> K		FAT	Uterus	TCGA-D1-A17Q-01	
1801	V -> G		FAT	CCLE	NCIH522_LUNG	
1811	R -> H		FAT	CCLE	QGP1_PANCREAS	
1818	R -> C		FAT	Stomach	TCGA-HU-A4GX-01	
1822	G -> V		FAT	CCLE	SNGM_ENDOMETRIUM	

1832	A -> T		FAT	COSMIC	COSMIC	
1836	A -> T		FAT	CCLE	IPC298_SKIN	
1836	A -> T		FAT	CCLE	RERFLCAD1_LUNG	
1837	T -> N		FAT	CCLE	NCIH522_LUNG	
1844	T -> A		FAT	Colorectal	587332	
1845	E -> K		FAT	Bladder	DS-bla-044	
1845	E -> K		FAT	Bladder	TCGA-LT-A5Z6-01	
1845	E -> K		FAT	Breast	Novartis	
1856	T -> I		FAT	Melanoma	TCGA-D3-A51H-06	
1857	E -> K		FAT	Liver	Novartis	
1857	E -> K		FAT	Melanoma	TCGA-EE-A3AG-06	
1866	Q -> R		FAT	COSMIC	COSMIC	
1888	F -> I		FAT	Kidney-ccRCC	TCGA-B0-4846-01	Current study, PMID: 24631838
1888	F -> L		FAT	Kidney-ccRCC	TCGA-CZ-4857-01	Current study, PMID: 24631838
1888	F -> L		FAT	Kidney-ccRCC	TCGA-CZ-4866-01	Current study, PMID: 24631838
1888	F -> V		FAT	Uterus	TCGA-BS-A0TC-01	Current study, PMID: 24631838
1888	F -> L		FAT	Uterus	TCGA-D1-A16X-01	Current study, PMID: 24631838
1890	R -> C		FAT	Colorectal	TCGA-AA-3663-01	
1890	R -> C		FAT	Melanoma	MEL-JWCI-WGS-1	
1890	R -> C		FAT	Melanoma	TCGA-FW-A3R5-06	
1894	L -> V		FAT	CCLE	SNU81_LARGE_INTE	
1899	N -> D		FAT	Colorectal	587332	
1903	T -> I		FAT	CCLE	ISHIKAWAHERAKLIO	
1905	R -> S		FAT	Breast	Novartis	
1907	L -> F		FAT	Colorectal	TCGA-AG-A002-01	
1912	D -> H	5734G>C	FAT	Kidney-ccRCC	Novartis RECORD-3	
1914	G -> C		FAT	COSMIC	COSMIC	
1921	E -> V		FAT	CCLE	CORL23_LUNG	
1948	T -> M		FAT	CCLE	GP2D_LARGE_INTES	
1950	R -> K		FAT	Melanoma	YUKIL	
1953	V -> L		FAT	COSMIC	COSMIC	
1966	R -> Q		FAT	Uterus	TCGA-D1-A167-01	
1970	Q -> E		FAT	Kidney-nccRCC	9267011	
1971	A -> T		FAT	Bladder	DS-bla-024	
1971	A -> T		FAT	Blood	CLL099	
1971	A -> T		FAT	Brain/CNS	TCGA-28-2502-01	

1971	A -> T	5911G>A	FAT	Kidney-ccRCC	Novartis RECORD-3	
1971	A -> S		FAT	Liver	H072999	
1973	I -> F		FAT	Breast	TCGA-E2-A15O-01	PMID: 24631838, 17360675
1973	I -> F		FAT	Kidney-ccRCC	TCGA-B0-5100-01	Current Study, PMID: 24631838, 17360675
1974	Y -> H		FAT	Breast	Novartis	
1974	Y -> H		FAT	CCLE	KMRC2_KIDNEY	
1974	Y -> C		FAT	Uterus	TCGA-D1-A1NU-01	
1977	T -> S		FAT	Blood	CLL005	PMID: 24631838
1977	T -> K		FAT	Kidney-ccRCC	TCGA-B0-4827-01	PMID: 24631838
1977	T -> K		FAT	Lymph	SU-DHL-9	PMID: 24631838
1977	T -> R		FAT	Prostate	TCGA-CH-5768-01	PMID: 24631838
1977	T -> K	5930C>A	FAT	Kidney-ccRCC	Novartis RECORD-3	
1981	K -> E		FAT	Breast	BR-V-049	
1981	K -> E		FAT	CCLE	MFE319_ENDOMETRIUM	
1986	A -> T		FAT	CCLE	TEN_ENDOMETRIUM	
1987	R -> W		FAT	Stomach	TCGA-D7-A4Z0-01	
1998	M -> I		FAT	COSMIC	COSMIC	
2006	V -> L		Kinase N lobe	CCLE	TUHR10TKB_KIDNEY	Current Study, PMID: 24631838
2006	V -> F		Kinase N lobe	Kidney-ccRCC	K104	PMID: 24631838
2006	V -> L		Kinase N lobe	Kidney-ccRCC	TCGA-CJ-4644-01	Current Study, PMID: 24631838
2006	V -> I		Kinase N lobe	Uterus	TCGA-B5-A11H-01	PMID: 24631838
2011	M -> V		Kinase N lobe	COSMIC	COSMIC	PMID: 20190810
2011	M -> I		Kinase N lobe	COSMIC	COSMIC	
2013	S -> G		Kinase N lobe	Uterus	TCGA-BG-A0MO-01	
2014	E -> K		Kinase N lobe	CCLE	UBLC1_URINARY_TR	PMID: 24625776
2016	L -> R		Kinase N lobe	CCLE	SNU738_CENTRAL_N	
2017	I -> T		Kinase N lobe	CCLE	BL41_HAEMATOPOIE	PMID: 18812319
2017	I -> T		Kinase N lobe	Kidney-nccRCC	TCGA-KM-8441-01	PMID: 18812319
2022	L -> P		FRB	COSMIC	COSMIC	
2023	W -> G		FRB	Lung	TCGA-66-2787-01	
2030	G -> V		FRB	CCLE	BCP1_HAEMATOPOIE	
2032	E -> K		FRB	Esophagus	TCGA-L5-A88W-01	

2033	E -> V		FRB	Kidney-ccRCC	TCGA-B0-4852-01	
2040	G -> E		FRB	Stomach	Novartis	
2047	M -> V		FRB	COSMIC	COSMIC	
2056	A -> V		FRB	Uterus	TCGA-B5-A11E-01	
2066	K -> R		FRB	Liver	H072999	
2077	D -> E		FRB	Melanoma	TCGA-EE-A2GC-06	
2088	Y -> D		FRB	Uterus	TCGA-AX-A0J0-01	
2100	A -> T		FRB	Lung	2334201	PMID: 24631838
2101	W -> L		FRB	Breast	TCGA-D8-A1Y0-01	
2106	H -> P	6317A>C	FRB	Kidney-ccRCC	Novartis RECORD-3	
2106	H -> Y		FRB	COSMIC	COSMIC	
2108	F - > L		FRB	Thyroid		PMID: 25295501
2125	Y -> C		Kinase N lobe	Liver	H090285	
2127	S -> F		Kinase N lobe	Colorectal	EV-061-P	
2134	R -> P		Kinase N lobe	Breast	COSMIC	
2134	R -> W		Kinase N lobe	COSMIC	COSMIC	
2134	R -> L		Kinase N lobe	Lung	TCGA-66-2754-01	PMID: 24631838
2141	P -> L		Kinase N lobe	Breast	Novartis	
2150	I -> V		Kinase N lobe	COSMIC	COSMIC	
2152	R -> C		Kinase N lobe	CCLE	A375_SKIN	PMID: 24631838
2152	R -> C		Kinase N lobe	Melanoma	TCGA-FW-A3R5-06	PMID: 24631838
2154	Q -> E		Kinase N lobe	COSMIC	COSMIC	
2155	S -> F		Kinase N lobe	Melanoma	TCGA-GF-A6C9-06	
2172	L -> M		Kinase N lobe	Head & neck	TCGA-DQ-7588-01	PMID: 24631838
2179	G -> E		Kinase N lobe	Melanoma	MEL-Ma-Mel-35	
2186	L -> V		Kinase N lobe	Cervix	TCGA-JW-A5VL-01	
2191	D -> H		Kinase N lobe	Cervix	TCGA-C5-A1BM-01	PMID: 24631838
2193	R -> C		Kinase N lobe	Stomach	TCGA-BR-4370-01	PMID: 24631838
2197	R -> C		Kinase N lobe	Esophagus	TCGA-XP-A8T6-01	
2198	H -> P		Kinase N lobe	Kidney-nRCC	Novartis RECORD-3	
2206	N -> S		Kinase N lobe	COSMIC	COSMIC	PMID: 24631838

2207	T -> I		Kinase N lobe	Melanoma	TCGA-EB-A5UN-06	
2209	L -> V		Kinase N lobe	Bladder	TCGA-BT-A0YX-01	PMID: 24631838
2209	L -> V	6625C>G	Kinase N lobe	Kidney-ccRCC	Novartis RECORD-3	
2210	A -> P		Kinase N lobe	Kidney-ccRCC	TCGA-B0-4810-01	PMID: 24631838
2210	A -> P	6628G>C	Kinase N lobe	Kidney-ccRCC	Novartis RECORD-3	
2215	S -> F		Kinase N lobe	Brain/CNS	P01_Rec	Current Study, PMID: 24631838, 24336570
2215	S -> T		Kinase N lobe	Brain/CNS	TCGA-06-1802-01	PMID: 24631838
2215	S -> Y		Kinase N lobe	CCLE	JHUEM7_ENDOMETRIUM	PMID: 24631838, 20190810
2215	S -> Y		Kinase N lobe	Cervix	TCGA-FU-A3HZ-01	PMID: 24631838, 20190810
2215	S -> F		Kinase N lobe	Cervix	TCGA-JW-A5VL-01	Current Study, PMID: 24631838, 24336570
2215	S -> Y		Kinase N lobe	Colorectal	TCGA-A6-6141-01	PMID: 24631838, 20190810
2215	S -> Y		Kinase N lobe	Colorectal	TCGA-AA-A00K-01	PMID: 24631838, 20190810
2215	S -> F		Kinase N lobe	Colorectal	TCGA-DM-A1D4-01	Current Study, PMID: 24631838, 24336570
2215	S -> F		Kinase N lobe	Colorectal	TCGA-F4-6806-01	Current Study, PMID: 24631838, 24336570
2215	S -> P		Kinase N lobe	COSMIC	COSMIC	PMID: 24631838
2215	S -> F		Kinase N lobe	Kidney-ccRCC	TCGA-CJ-5679-01	Current Study, PMID: 24631838, 24336570
2215	S -> F	6644C>T	Kinase N lobe	Kidney-ccRCC	Novartis RECORD-3	
2215	S -> Y	6644C>A	Kinase N lobe	Kidney-ccRCC	Novartis RECORD-3	
2215	S -> Y		Kinase N lobe	Kidney-nccRCC	9266804	PMID: 24631838, 20190810
2215	S -> Y		Kinase N lobe	Kidney-nccRCC	TCGA-A4-7828-01	PMID: 24631838, 20190810
2215	S -> F		Kinase N lobe	Melanoma	MEL-UKRV-Mel-20	Current Study, PMID: 24631838, 24336570
2215	S -> F		Kinase N lobe	Melanoma	YULAN	Current Study, PMID: 24631838, 24336570
2215	S -> Y		Kinase N lobe	Uterus	TCGA-BG-A0VX-01	PMID: 24631838, 20190810
2215	S -> Y		Kinase N lobe	Uterus	TCGA-BS-A0UF-01	PMID: 24631838, 20190810

2215	S -> Y		Kinase N lobe	Uterus	TCGA-BS-A0UV-01	PMID: 24631838, 20190810
2216	L -> P		Kinase N lobe	Brain/CNS	TCGA-CS-5396-01	PMID: 24631838
2217	R -> W		Kinase N lobe	CCLE	HEC251_ENDOMETRIUM	PMID: 24631838
2220	L -> F		Kinase N lobe	Kidney-ccRCC		Current study, PMID: 24631838
2223	Q -> K		Kinase N lobe	Colorectal	TCGA-A6-4105-01	Current study
2223	Q -> K		Kinase N lobe	Kidney-ccRCC		Current study, PMID: 24631838, 24622468
2225	Y -> C		Kinase N lobe	Esophagus	TCGA-VQ-A8PE-01	
2226	A -> S		Kinase N lobe			PMID: 24631838
2228	I -> T		Kinase N lobe	Kidney-ccRCC	TCGA-B0-5098	Current study, PMID: 24631838
2230	L -> V		Kinase N lobe	Kidney-ccRCC	TCGA-CJ-4887-01	Current study, PMID: 24631838
2231	S -> W		Kinase N lobe	CCLE	SNU1196_BILIARY_	PMID: 24631838
2232	T -> I		Kinase N lobe	CCLE	KMH2_HAEMATOPOIE	PMID: 24631838
2238	G -> D		Kinase N lobe	CCLE	CW2_LARGE_INTEST	PMID: 24631838
2239	W -> C		Kinase N lobe	Cervix	TCGA-JW-A5VL-01	
2240	V -> G		Kinase N lobe	COSMIC	COSMIC	
2241	P -> S		Kinase C lobe	Bladder	DS-bla-084	
2241	P -> S		Kinase C lobe	Bladder	TCGA-DK-A6B6-01	
2241	P -> S		Kinase C lobe	Cervix	TCGA-JW-A5VL-01	
2241	P -> H	6722C>A	Kinase C lobe	Kidney-ccRCC	Novartis RECORD-3	
2251	R -> Q		Kinase C lobe	Lung	TCGA-97-7554-01	
2254	R -> M		Kinase C lobe	CCLE	HEC1A_ENDOMETRIUM	
2260	L -> H		Kinase C lobe	Head & neck	HN_62421	
2265	H -> P		Kinase C lobe	CCLE	SNU520_STOMACH	
2266	R -> P		Kinase C lobe	Lung	TCGA-75-5126-01	
2268	M -> V		Kinase C lobe	COSMIC	COSMIC	
2272	A -> S		Kinase C lobe	Lung	TCGA-34-5239-01	

2272	A -> V		Kinase C lobe	Melanoma	TCGA-EB-A3Y7-01	
2294	T -> A		Kinase C lobe	Stomach	TCGA-BR-8363-01	
2311	E -> K		Kinase C lobe	Bladder	DS-bla-037	
2327	M -> I		Kinase C lobe	Brain/CNS	TCGA-DU-6393-01	Current study
2327	M -> I		Kinase C lobe	Kidney-ccRCC	TCGA-A3-3347-01	Current study
2333	I -> M		Kinase C lobe	Colorectal	TCGA-AA-3666-01	
2334	L -> V		Kinase C lobe	Kidney-ccRCC	TCGA-B0-5691-01	PMID: 24631838
2338	D -> N		Kinase C lobe	Esophagus	TCGA-2H-A9GR-01	
2340	H -> R		Kinase C lobe	CCLE	L540_HAEMATOPOIE	
2345	M -> V		Kinase C lobe	CCLE	NCIH446_LUNG	
2351	G -> E		Kinase C lobe	Esophagus	ESCC-148T	
2355	H -> R		Kinase C lobe	Lung	LUAD-FH5PJ	
2368	R -> Q		Kinase C lobe	CCLE	HEC108_ENDOMETRIUM	
2369	E -> K		Kinase C lobe	COSMIC		
2388	E -> Q		Kinase C lobe	Breast	TCGA-BH-A0HP-01	
2400	C -> Y		Kinase C lobe	Lung	585223	
2406	V -> M		Kinase C lobe	COSMIC	COSMIC	
2406	V -> A		Kinase C lobe	Kidney-ccRCC		Current study PMID:21248752
2412	D -> H		Kinase C lobe	COSMIC	COSMIC	
2412	D -> V		Kinase C lobe	Liver	H061142	
2413	S -> I	7238G>T	Kinase C lobe	Kidney-ccRCC	Novartis RECORD-3	
2414	V -> I		Kinase C lobe	Lymph	OCI-Ly1	
2416	A -> V		Kinase C lobe	COSMIC	COSMIC	
2417	V -> M		Kinase C lobe	Colorectal	587338	
2417	V -> M		Kinase C lobe	Kidney-ccRCC	K31	
2419	E -> K		Kinase C lobe	Cervix	TCGA-EK-A3GK-01	PMID: 24631838, 24625776, 17360675

2419	E -> K	7255G>A	Kinase C lobe	Kidney-ccRCC	Novartis RECORD-3	
2420	A -> P		Kinase C lobe	Blood	CLL147	
2420	A -> V		Kinase C lobe	Melanoma	TCGA-FS-A4FC-06	
2422	V -> I		Kinase C lobe	COSMIC	COSMIC	
2424	D -> H		Kinase C lobe	COSMIC	COSMIC	
2424	D -> N		Kinase C lobe	Melanoma	TCGA-ER-A42L-06	
2427	L -> Q		Kinase C lobe	Brain/CNS	TCGA-06-0122-01	
2427	L -> R		Kinase C lobe	CCLE	ST486_HAEMATOPOI	
2427	L -> P		Kinase C lobe	Kidney-ccRCC		PMID: 25159823
2427	L -> Q	7280T>A	Kinase C lobe	Kidney-ccRCC	Novartis RECORD-3	
2427	L -> Q		Kinase C lobe	Kidney-nccRCC	9266792	
2427	L -> R		Kinase C lobe	Kidney-nccRCC	TCGA-KN-8437-01	
2430	R -> M		Kinase C lobe	CCLE	MOLT16_HAEMATOPO	PMID: 24631838
2431	L -> P		Kinase C lobe	Kidney-ccRCC		Current study, PMID: 24631838, 22397650
2441	R -> Q		Kinase C lobe	Colorectal	TCGA-G4-6322-01	
2457	I -> M		Kinase C lobe	Colorectal	587376	
2458	L -> V		Kinase C lobe	Breast	Novartis	
2476	P -> L		Kinase C lobe	COSMIC	COSMIC	PMID: 20190810
2488	V -> G		Kinase C lobe	Eye	TCGA-RZ-AB0B-01	
2490	P -> A		Kinase C lobe	CCLE	L1236_HAEMATOPOI	
2500	I -> F		Kinase C lobe	Brain/CNS	TCGA-QR-A6GX-01	PMID: 24631838
2500	I -> N		Kinase C lobe	Breast	Novartis	
2500	I -> F		Kinase C lobe	Breast	TCGA-A8-A06Y-01	PMID: 24631838
2500	I -> F		Kinase C lobe	CCLE	JHOM2B_OVARY	PMID: 24631838
2500	I -> M		Kinase C lobe	Kidney-ccRCC	TCGA-CW-5580-01	PMID: 24631838
2500	I -> M		Kinase C lobe	NCI60	HCC_2998	PMID: 24631838

2500	I -> M		Kinase C lobe	Stomach	TCGA-BR-8680-01	PMID: 24631838
2500	I -> M		Kinase C lobe	Uterus	TCGA-B5-A0JY-01	PMID: 24631838
2501	I -> F		Kinase C lobe	Eye	TCGA-RZ-AB0B-01	PMID: 17360675
2501	I -> F	7501A>T	Kinase C lobe	Kidney-ccRCC	Novartis RECORD-3	
2501	I -> F		Kinase C lobe	Liver	TCGA-DD-A11A-01	PMID: 17360675
2505	R -> Q		Kinase C lobe	COSMIC	COSMIC	PMID: 24631838
2505	R -> L		Kinase C lobe	COSMIC	COSMIC	
2505	R -> P		Kinase C lobe	Kidney-ccRCC		Current study, PMID: 24631838, 20190810
2509	T -> A		Kinase C lobe	CCLE	COLO684_ENDOMETR	
2509	T -> A		Kinase C lobe	CCLE	COLO704_OVARY	
2511	R -> Q		Kinase C lobe	Bladder	B16	PMID: 24631838
2512	D -> H		Kinase C lobe	COSMIC	COSMIC	PMID: 24631838
2512	D -> Y		Kinase C lobe	Uterus	TCGA-AP-A0LL-01	PMID: 24631838
2512	D -> G		Kinase C lobe	Uterus	TCGA-AX-A0J1-01	PMID: 24631838
2523	T -> M		Kinase C lobe	Uterus	TCGA-D1-A167-01	
2524	Q -> L		Kinase C lobe	COSMIC	COSMIC	
2526	E -> K		Kinase C lobe	Cervix	TCGA-IR-A3LL-01	
2532	A -> V		Kinase C lobe	Stomach	TCGA-BR-4292-01	

* For Novartis RECORD-3 data

Supplementary Table 2. Summary of phenotypes of WT mTOR and selected mTOR mutants characterized in current study.

mTOR	WT	A1105P	L1460P	C1483F	F1888L	T1977K	S2215F	L2230V	M2327I	R2505P
PRAS40 overexpression	Sensitive	N/A	Sensitive	Sensitive	Sensitive	Sensitive	Sensitive	Sensitive	Sensitive	Sensitive
RHEB knockdown	Sensitive	N/A	Sensitive	Sensitive	Sensitive	Sensitive	Sensitive	Sensitive	Sensitive	N/A
Rag mutant overexpression	Sensitive	N/A	Sensitive	Sensitive	Sensitive	Sensitive	Sensitive	Sensitive	Sensitive	Sensitive
Serum deprivation	Sensitive	N/A	Partially Resistant	Partially Resistant	Partially Resistant	Partially Resistant	Partially Resistant	Partially Resistant	N/A	N/A
Glucose deprivation	Sensitive	N/A	Partially Resistant	Partially Resistant	Partially Resistant	Partially Resistant	Partially Resistant	Partially Resistant	N/A	N/A
Amino acid deprivation	Sensitive	N/A	Sensitive	Sensitive	Sensitive	Sensitive	Sensitive	Sensitive	N/A	N/A
FKBP38 knockdown	No effect	N/A	No effect	No effect	No effect	No effect	No effect	No effect	No effect	No effect
FKBP38 overexpression	No effect	N/A	No effect	No effect	No effect	No effect	No effect	No effect	No effect	No effect
Binding with DEPTOR	Normal	N/A	Reduced	Reduced	Normal	Normal	Normal	Normal	Normal	Reduced
DEPTOR overexpression	Sensitive	N/A	Sensitive	Sensitive	Resistant	Resistant	Resistant	Resistant	Resistant	Resistant
Vmax	Normal	N/A	N/A	N/A	N/A	N/A	Increased	Increased	N/A	N/A
Km	Normal	N/A	N/A	N/A	N/A	N/A	Reduced	Normal	N/A	N/A
RAPTOR overexpression	Sensitive	N/A	Resistant	Resistant	Sensitive	Resistant	Resistant	Sensitive	Sensitive	Sensitive
REDD1 overexpression	Sensitive	N/A	Resistant	Resistant	Sensitive	Resistant	Resistant	Resistant	Resistant	Resistant
Rapamycin 10 nM	Sensitive	N/A	N/A	Sensitive	Sensitive	Sensitive	Sensitive	Sensitive	N/A	N/A
Rapamycin 2.5 nM	Sensitive	N/A	N/A	Sensitive	Sensitive	Sensitive	Sensitive	Sensitive	N/A	N/A
Tumor growth using Vhl-silenced NIH/3T3	No	No	N/A	Yes	Yes	Yes	Yes	Yes	N/A	Yes

Supplementary Table 2 (continue). Summary of phenotypes of WT mTOR and selected mTOR mutants characterized in current study.

mTOR	C1483F/ T1977K	C1483F/ S2215F	T1977K/ S2215F	F1888L/ L2230V
PRAS40 overexpression	Sensitive	Sensitive	Sensitive	Sensitive
RHEB knockdown	Resistant	Resistant	Resistant	Resistant
Rag mutant overexpression	Resistant	Resistant	Resistant	Resistant
Serum deprivation	Resistant	Resistant	Resistant	Resistant
Glucose deprivation	Resistant	Resistant	Resistant	Resistant
Amino acid deprivation	Partially resistant	Partially resistant	Partially resistant	Partially resistant
Rapamycin 10 nM	N/A	Sensitive	N/A	Sensitive
Rapamycin 2.5 nM	N/A	Partially resistant	N/A	Partially resistant

Supplementary Table 3. List of primers used for site-directed mutagenesis

mTOR K860N	5’-GAG CCC TAC AGG AAT TAC CCT ACT TTG C-3’
mTOR E919V	5’-GTC AGC CTG TCA GTA TCC AAG TCA AGT C-3’
mTOR A1105P	5’-CCA GCT GTT TGG CCC CAA CCT GGA TGA C-3’
mTOR L1443S	5’-GCG GCC GGA GTG TCA GAA TAT GCC ATG AAA C-3’
mTOR A1459P	5’-CAC GAG TGG GAG GAT CCC CTT GTG GCC TAT G-3’
mTOR L1460P	5’-GTG GGA GGA TGC CCC TGT GGC CTA TGA CAA G-3’
mTOR C1483F	5’-GGG CCG CAT GCG CTT CCT CGA GGC CTT GGG-3’
mTOR F1888L	5’-GCC GTC CAG GGC TTG TTC CGT TCC ATC TCC-4’
mTOR F1888I	5’-CTG CCG TCC AGG GCA TCT TCC GTT CCA TCT C-3’
mTOR F1888V	5’-CTG CCG TCC AGG GCG TCT TCC GTT CCA TCT C-3’
mTOR I1973F	5’-CCC CCA GGC CCT CTT CTA CCC ACT GAC AG-3’
mTOR T1977K	5’-CAT CTA CCC ACT GAA AGT GGC TTC TAA GTC-3’
mTOR V2006L	5’-CAC AGC AAC ACC CTG CTC CAG CAG GCC ATG-3’
mTOR S2215F	5’-CCA ATG ACC CAA CAT TTC TTC GGA AAA ACC-3’
mTOR L2220F	5’ CAT CTC TTC GGA AAA ACT TCA GCA TCC AGA G-3’
mTOR Q2223K	5’-GGA AAA ACC TCA GCA TCA AGA GAT ACG CTG TC-3’
mTOR I2228T	5’-GAG ATA CGC TGT CAC CCC TTT ATC GAC C-3’
mTOR L2230V	5’-CGC TGT CAT CCC TGT ATC GAC CAA CTC GG-3’
mTOR M2327I	5’-GTT CTT TAG CGG TCA TAT CAA TGG TTG GG-3’
mTOR V2406A	5’-CAC AGT GAT GGA GGC GCT GCG AGA GCA C-3’
mTOR L2431P	5’-GCT GAA CTG GAG GCC GAT GGA CAC AAA TAC C-3’
mTOR R2505P	5’-GAT TAT TAA CAG GGT TCC AGA TAA GCT CAC TGG-3’
Akt1 E17K	5’-GGC TGC ACA AAC GAG GGA AAT ATA TTA AAA CCT GGC -3’

SUPPLEMENTARY METHODS

Plasmid Construction, shRNA, siRNA, antibodies

pcDNA3-Flag-mTOR was a gift from Jie Chen (Addgene plasmid # 26603). The following plasmids were gifts from David Sabatini: pRK5-HA-RAPTOR (Addgene plasmid # 8513), pRK5-HA-PRAS40 (Addgene plasmid # 15481), pRK5-HA-GST-RAGB (Addgene plasmid # 19301), pRK5-HA-GST-RAGD (Addgene plasmid # 19307), pRK5-HA-GST-RAGB^{GDP} (Addgene plasmid # 19302), pRK5-HA-GST-RAGD^{GTP} (Addgene plasmid # 19309), and pRK5-HA-GST-RHEB (Addgene plasmid # 14951), pRK5-HA-GST-Presc-mAkt1 (Addgene plasmid # 48805), non-degradable pRK5-Flag-DEPTOR (13xS/T->A) (Addgene plasmid #21702), HA-GST-tagged S6K1 (pRK5-HA-GST-S6K1). HA-tagged 4EBP1 (pcDNA3-HA-4EBP1) was constructed by inserting a BamHI-SalI fragment containing HA-4EBP1 from pBABE-HA-4EBP1 (1) into the BamHI-XhoI sites of pcDNA3. HA-GST tagged GFP (pRK5-HA-GST-GFP) was constructed by swapping a NotI-SalI fragment containing GFP from pEGFP-N3 (Clontech) with that of RHEB from pRK5-HA-GST-RHEB. HA-tagged REDD1 (pcDNA3-HA-REDD1) was constructed by amplifying the REDD1 gene from a human cDNA library and cloned into the BglII and XhoI sites of pcDNA3-HA. pLenti-REDD1 was constructed by inserting a BglII-XhoI fragment containing REDD1 from pcDNA3-HA-REDD1 into the BamHI-XhoI sites of pLenti-CMV-Blast empty(Addgene plasmid #17486, a gift from Eric Campeau). HA-tagged FKBP38 (pcDNA3-HA-FKBP38) was constructed by amplifying the FKBP38 gene from a mouse cDNA library and cloned into the BglII and XhoI sites of pcDNA3-HA.

Lentiviral shRNA constructs pLKO.1-shRHEB1 (Target sequence: 5'-CCTCAGACATACTCCATAGAT-3') was a gift from Kun-Liang Guan (Addgene plasmid # 26625). Lentiviral shRNA constructs pLKO.1-shmVhl (Target Sequence: 5' TCTCAGGTCATCTTCTGCAAT-3') was obtained from Sigma (TRCN0000009735). Lentiviral shRNA constructs pLKO.1-shmVhl(2) (Target Sequence: 5' GTTAACCAAACGGAGCTGTTT-3')

was obtained from Sigma (TRCN0000009737). Lentiviral shRNA constructs pLKO.1-shMTOR (Target Sequence: 5' GCTGCTGTTGAAGAATATATT-3') was obtained from Sigma (TRCN0000039783) Inducible lentiviral shRNA construct Tet-pLKO-puro-shFKBP38 was constructed by inserting the annealed oligos (5'-CCGGTGAAGGTGAAGTGTCTGAACACTCGAGTGTTCAGACACTTCACCTTCATTTTTG -3' and 5'-AATTCAAAAATGAAGGTGAAGTGTCTGAACACTCGAGTGTTCAGACACTTCACCTTCA-3') into the EcoRI and AgeI sites of Tet-pLKO-puro (a gift from Dmitri Wiederschain, Addgene plasmid # 21915).

siGenome SMARTpool siRNA targeting mouse Redd1 (Target Sequence: 5' GUGCCCACCUUUCAGUUGA-3', 5' GCUAAGUACCGGCUUCAGA-3', 5' GCUGUUAAGUUCUGCCAAC-3', 5' GAUCGUUUCUCGUCCUCCU-3') was obtained from Dharmacon (M-056656). The scramble siRNA oligonucleotides were purchased from Dharmacon (D-001206-13-20);

Antibodies used for immunoblot analysis are as follows: anti-pThr-389 S6K (no. 9205, Cell Signaling Technology), anti-S6K (no. 9202, Cell Signaling Technology), anti-pSer-65 4EBP1 (no. 9451, Cell Signaling Technology), anti-4EBP1 (no. 9452, Cell Signaling Technology), anti-pSer-473 AKT1 (no. 9271, Cell Signaling Technology), anti-AKT1 (no. 9272, Cell Signaling Technology), anti-pSer 235/236 S6 (no. 4858, Cell Signaling Technology), anti-S6 (no. 2217, Cell Signaling Technology), anti-pSer 939 TSC2 (no. 3615, Cell Signaling Technology), anti-TSC2 (no. 4308, Cell Signaling Technology), anti-HA (12CA5), anti-mTOR (no. 2972, Cell Signaling Technology), anti-RAPTOR (no. 2280, Cell Signaling Technology), anti-RICTOR (A300-459A, Bethyl Laboratories),anti-DEPTOR (no.11816, Cell Signaling Technology), anti- PRAS40 (no. 2610, Cell Signaling Technology), anti-VHL (no. 2738, Cell Signaling Technology), anti-Flag (F1804, Sigma), anti-RHEB (ab25873, Abcam), anti-FKBP38

(AF3580, R&D system), anti-Flag M2 Affinity Gel (A2220, Sigma), anti-HA agarose (A2095, Sigma), anti-REDD1 (no. 10638-1-AP, Protein Tech), anti-β-Actin (A-1978, Sigma). The dilution for all of the primary antibodies for immunoblot analysis was 1/1,000, except for β-Actin, which is 1/10,000. The dilution for all of the secondary antibodies for immunoblot analysis was 1/5,000.

Generation of tetracycline-inducible HeLa and NIH/3T3 cell lines expressing wild-type or mutant mTOR

HeLa cells were first infected with retrovirus expressing rtTA3 (pMSCV-rtTA3-PGK-hygro), followed by selection with hygromycin at 500 μg/ml. The selected cells were subsequently infected with retrovirus expressing TRE-Flag tagged wild-type or mutant mTOR, followed by selection with puromycin at 2 μg/ml. The tet-inducible mTOR expressing HeLa cell lines were cultured in DMEM (Invitrogen) supplemented with 10% Tet-approved FBS (Clontech), non-essential amino acids, L-glutamine, sodium pyruvate, antibiotics (Invitrogen), 50 μg/ml hygromycin, and 0.1 μg/ml puromycin. Optimized addition of doxycycline between 0.5-2 μg/ml in the culture medium is required to achieve equal expression of Flag-tagged wild-type and mutant mTOR. The tet-inducible vector was constructed by the Scott Lowe Lab (Memorial Sloan-Kettering Cancer Center, New York).

NIH/3T3 cells were first infected with retrovirus expressing rtTA3 (pMSCV-rtTA3-PGK-hygro), followed by selection with hygromycin at 500 μg/ml. The selected cells were subsequently infected with lentivirus expressing shRNA construct targeting either Vhl or luciferase, followed by selection with puromycin at 2 μg/ml. The selected cells were subsequently infected with retrovirus expressing TRE-Flag tagged wild-type or mutant mTOR and IRES-GFP, followed by addition of doxycycline to induce expression of Flag-tagged mTOR-IRES-GFP. GFP-positive cells were sorted using MoFlo (Beckman Coulter). The sorted

NIH/3T3 cell lines expressing shRNA constructs and the tet-inducible mTOR-IRES-GFP were cultured in DMEM (Invitrogen) supplemented with 10% Tet-approved FBS (Clontech), non-essential amino acids, L-glutamine, sodium pyruvate, antibiotics (Invitrogen), 50 μg/ml hygromycin, and 0.1 μg/ml puromycin. Optimized addition of doxycycline between 0.5-2 μg/ml in the culture medium is required to achieve equal expression of Flag-tagged wild-type and mutant mTOR. To overexpress REDD1 in NIH/3T3 cells expressing shVhl and mutant mTOR constructs, the cells were infected with lentivirus expressing construct expressing either empty vector or REDD1, followed by selection with blasticidin at 2 μg/ml for 1 weeks.

Co-immunoprecipitation

$8x10^6$ 293T cells were seeded in a 10 cm dish, transfected 24 hours later with 10 μg of vectors expressing Flag-tagged wild-type or mutant mTOR as described above. 48 hours post-transfection, cells were harvested in ice-cold PBS buffer. For co-immunoprecipitation of mTOR with endogenous DEPTOR, cell pellets were lysed in buffer 1 (20 mM HEPES pH 7.4, 2 mM EDTA, and 0.3% CHAPS) containing complete protease inhibitor (Roche) and phosphatase inhibitors (EMD/Millipore). Whole cell lysates (500 μg protein) were incubated with anti-Flag M2 agarose (Sigma) overnight, then washed three times with buffer 1, and subjected to NuPAGE electrophoresis and immunoblot analysis. For co-immunoprecipitation of mTOR with other proteins, cells were lysed in buffer 2 (50mM HEPES pH7.4, 2 mM EDTA, 0.3% CHAPS, and 40 mM NaCl), whole cell lysates were incubated with anti-Flag M2 agarose for 3 hours, and then washed three times with buffer 2 containing 300 mM NaCl.

In vitro kinase assays

For immunoprecipitation of mTORC1 for in vitro kinase assays, cells were lysed in buffer 3 (40mM HEPES pH7.4, 2 mM EDTA, 0.3% CHAPS), whole cell lysates were incubated with anti-Flag M2 agarose for 3 hours, and then washed three times with buffer 3 containing 150 mM

NaCl and one time with wash buffer (50mM HEPES pH7.4, 150 mM KCl). To purify S6K for in vitro kinase assays, $8x10^6$ 293T cells were seeded in a 10 cm dish for 24 hours, transfected with 10 µg of vectors expressing HA-tagged S6K as described above. 48 hours post-transfection, cells were treated with BEZ-235 (10µM) for 1 hour and harvested in ice-cold PBS buffer. Cells were lysed in NP-40 buffer (150 mM NaCl, 1% NP-40, and 50mM Tris-Cl, pH8.0) containing complete protease inhibitor (Roche) and phosphatase inhibitors (EMD/Millipore). Whole cell lysates (500 µg) were incubated with anti-HA agarose (Sigma) for 3 hours, then washed five times with NP-40 buffer, and elute with HA peptide.

Purified Flag-tagged mTORC1 complex containing wild-type or mutant mTOR was incubated with purified HA-S6K in the Kinase buffer (25mM HEPES pH7.4, 50mM KCl, 10mM $MgCl_2$) in a final volume of 13.5 µl on ice for 10 min, followed by the addition of 1.5 µl of ATP (final concentration 0.5 mM) and incubation at 30°C for 30 min. The reaction was terminated by adding 2X NuPAGE LDS sample buffer (Invitrogen) and heated at 100°C for 2 min, and subjected to immunoblot analysis as described above.

Targeted gene sequencing

Paraffin-embedded patient samples including tumors (archival tissues, 260 patients) and adjacent normal kidney tissue (181 patients) from RECORD-3 trial were macro dissected and subjected to DNA extraction. A dedicated genitourinary pathologist reviewed all sections and selected areas of tumor and healthy tissue for macro dissection and DNA extraction. Somatic mutations in exons of 341 cancer related genes were identified by an NGS assay (MSK IMPACT platform) (2) at ~530X coverage. mTOR missense mutations are reported here.

Molecular dynamics simulations

The canonical wild-type mTOR sequence for the UniProt-annotated PI3K/PI4K domain span (residues 2182-2516) was modeled onto the X-ray structure of mTOR from chain A of

RCSB entry 4JSN using the Ensembler automated simulation setup tool (3) with default parameters. All residues were assigned default protonation states typical of pH 7.4. The AMBER 99SB-ILDN (4) forcefield was used for the protein along with the TIP3P solvent model (5) with neutralizing monovalent Na+ or Cl- counterions. The resulting simulation box had 80,983 atoms. The OpenMM 6.2 simulation package (6) was used for all minimization, equilibration, and production simulations. Equilibration simulations utilized Langevin dynamics with a timestep of 2 fs and collision rate of 20/ps, along with a Monte Carlo barostat with molecular scaling and update interval of 50 steps, with temperature and pressure control set to 300 K and 1 atm. Particle-mesh Ewald (PME) with default parameters was used for long-range electrostatic treatment, direct-space and Lennard-Jones interactions were truncated at 9 A, and a long-range dispersion correction was employed. Bonds to hydrogen were constrained using CCMA (7) using the default tolerance of 1e-5, and waters were rigidly constrained using SETTLE (8). The Ensembler package (9) handles energy minimization and refinement in implicit solvent followed by a short minimization and equilibration step in explicit solvent prior to production simulations.

Production simulations of the wild-type kinase domain were run on Folding@home (10) using a simulation core based on OpenMM 6.2 and the same simulation parameters, with the exception of a reduced collision rate of 1/ps. The structure obtained after 589.5 ns---which had relaxed much of the initial loop-modeling-induced structural artifacts---was used as a starting model for further modeling of mutations and subsequent production simulations.

To model mTOR mutants and wild-type kinase domain behavior, PDBFixer v1.2 (11), part of the Omnia molecular simulation suite (12), was used to generate mutant versions of the mTOR kinase domain using the relaxed wild-type structure. Subsequent simulation steps utilized reaction-field electrostatics with a cutoff of 10A in place of PME to allow longer trajectories to be generated. Proteins were resolved in TIP3P water with NaCl counterions to

neutralize the system and produce an environment of approximately 150 mM NaCl to using a padding of 11A around the kinase, resulting in systems of approximately 81K atoms. Langevin dynamics with a collision rate of 5/ps was used for subsequent production simulations of mutant and wild-type kinase domains, which also employed a simulation core based on OpenMM 6.2 on Folding@home. Simulation boxes were energy minimized with the OpenMM LocalEnergyMinimizer facility before subjecting them to subsequent dynamics.

Ten replicate simulations of each mutant simulation box were run on Folding@home, with each replicate receiving a unique random number seed ensuring rapid decorrelation of trajectories. Nine out of ten trajectories were 501 nanoseconds of simulation, and one trajectory was 471 nanoseconds long. The initial 100 ns of each simulation were discarded and subsequent simulation data was analyzed for structural alternations indicative of rapid mutation-induced conformational changes.

Conformational changes were detected by generating a contact map, which shows the net change in the probability of forming a contact between a pair of residues from wild-type to mutant. To calculate these probabilities, mdtraj (13) was first used to calculate the distance between every residue pair based on the closest heavy atoms in each frame of the simulations after 100 ns. Using 5 angstroms as the threshold at which a contact was formed, the number of frames in which a contact was formed was divided by the total number of frames for each simulation, giving a probability for each residue pair in that simulation which could be averaged over the number of replicates per mutant. The wild-type probability was subtracted from the mutant, giving a net change in probability to form a contact for each residue pair in the protein. The structural images were generated using PyMOL to visually inspect areas of interest identified by the contact map over the course of each simulation.

The individual net changes in average contact probabilities following 100 ns of relaxation were computed as the difference in average contact probabilities between mutant and wild-type simulations. For each kinase, the average contact probability was computed as the fraction of snapshots in which the contact was made, where all frames (after discarding the initial 100 ns/trajectory) were averaged over the ten replicate trajectories initiated from each kinase mutant or wild-type simulation box using different initial velocities and random number seeds. The net change in probabilities are reported plus or minus a standard error, which is calculated as stddev/sqrt(N), where N=10 is the number of replicate trajectories.

SUPPLEMENTARY REFERNCE

1. She QB, Halilovic E, Ye Q, Zhen W, Shirasawa S, Sasazuki T, Solit DB, and Rosen N. 4E-BP1 is a key effector of the oncogenic activation of the AKT and ERK signaling pathways that integrates their function in tumors. *Cancer cell.* 2010;18(1):39-51.
2. Cheng DT, Mitchell TN, Zehir A, Shah RH, Benayed R, Syed A, Chandramohan R, Liu ZY, Won HH, Scott SN, et al. Memorial Sloan Kettering-Integrated Mutation Profiling of Actionable Cancer Targets (MSK-IMPACT): A Hybridization Capture-Based Next-Generation Sequencing Clinical Assay for Solid Tumor Molecular Oncology. *The Journal of molecular diagnostics : JMD.* 2015;17(3):251-64.
3. Chodera JD. A simple method for automated equilibration detection in molecular simulations. *BioRxiv.* 2015.
4. Lindorff-Larsen K, Piana S, Palmo K, Maragakis P, Klepeis JL, Dror RO, and Shaw DE. Improved side-chain torsion potentials for the Amber ff99SB protein force field. *Proteins.* 2010;78(8):1950-8.
5. Jorgensen WL, Chandrasekhar J, Madura JD, Impey RW, and Klein ML. Comparison of simple potential functions for simulating liquid water. *J Chem Phys* 1983;79(
6. Eastman P, Friedrichs MS, Chodera JD, Radmer RJ, Bruns CM, Ku JP, Beauchamp KA, Lane TJ, Wang LP, Shukla D, et al. OpenMM 4: A Reusable, Extensible, Hardware Independent Library for High Performance Molecular Simulation. *Journal of chemical theory and computation.* 2013;9(1):461-9.
7. Eastman P, and Pande VS. CCMA: A Robust, Parallelizable Constraint Method for Molecular Simulations. *Journal of chemical theory and computation.* 2010;6(2):434-7.
8. Miyamoto S, and Kollman PA. Settle: An analytical version of the SHAKE and RATTLE algorithm for rigid water models. *Journal of computational chemistry.* 1992;13(8):952-62.
9. Parton DL, Chodera JD, and Grinaway PB. https://github.com/choderalab/ensembler.
10. Shirts M, and Pande VS. COMPUTING: Screen Savers of the World Unite! *Science.* 2000;290(5498):1903-4.
11. Li Y, Wang R, Ma E, Deng Y, Wang X, Xiao J, and Jing Y. The induction of G2/M cell-cycle arrest and apoptosis by cucurbitacin E is associated with increased phosphorylation of eIF2alpha in leukemia cells. *Anti-cancer drugs.* 2010;21(4):389-400.

12. Misra UK, and Pizzo SV. Modulation of the unfolded protein response in prostate cancer cells by antibody-directed against the carboxyl-terminal domain of GRP78. *Apoptosis : an international journal on programmed cell death.* 2010;15(2):173-82.
13. McGibbon RT, Beauchamp KA, Harrigan MP, Klein C, Swails JM, Hernandez CX, Schwantes CR, Wang LP, Lane TJ, and Pande VS. MDTraj: A Modern Open Library for the Analysis of Molecular Dynamics Trajectories. *Biophysical journal.* 2015;109(8):1528-32.